

~~HYDROLOGICAL AND PEDOLOGICAL EFFECTS OF COMBINING ITALIAN ALDER AND BLACKBERRIES IN AN AGROFORESTRY WINDBREAK SYSTEM IN SOUTH AFRICA~~

Hydrological and pedological effects of combining Italian alder and blackberries in an agroforestry windbreak system in South Africa

Svenja Hoffmeister¹, Rafael Bohn Reckziegel², Ben du Toit³, Sibylle K. Hassler^{1,4}, Florian Kestel⁵, Rebekka Maier², Jonathan P. Sheppard², Erwin Zehe¹

¹Institute ~~for of~~ Water and ~~River Basin Management~~Environment, Karlsruhe Institute of Technology, Karlsruhe, 76131, Germany

²Institute of Forest Sciences, University of Freiburg, Freiburg, 79106, Germany

³Department of Forest and Wood Science, Stellenbosch University, Stellenbosch, 7602, South Africa

⁴Institute for Meteorology and Climate Research, Atmospheric Trace Gases and Remote Sensing, Karlsruhe Institute of Technology, Eggenstein-Leopoldshafen, 76344, Germany

⁵Working Group: Soil Erosion and Feedback in Research Area 1 “Landscape Functioning”, Leibniz Centre for Agricultural Landscape Research, Müncheberg, 15374, Germany

Correspondence to: Svenja Hoffmeister (svenjahoffmeister@gmail.com)

Abstract. The Western Cape in South Africa is a water scarce region which ~~under forecasted climate change scenarios may will~~ likely receive less rainfall and higher air temperatures ~~under projected climate change scenarios~~. The integration of trees within agricultural systems provides an effective measure for improving water retention on agricultural land. Studying an established ~~and~~ irrigated agroforestry system (AFS) combining alder (*Alnus cordata* (Loisel.) Duby) as a linear windbreak with a blackberry (*Rubus fruticosus* L.) crop, we explore the water use dynamics of the intercrop as influenced by the windbreak element by combining methods from hydrology, soil science and forestry. ~~We also aim~~ disciplines. Our objective is to evaluate explore whether the ~~proposed experimental design is sufficient to capture~~ AFS positively impacts the water balance ~~and by combining measurement campaigns to characterise~~ the ~~underlying control~~ spatial variability of various key system properties with continuous monitoring.

~~Due~~ The campaigns encompassed extensive soil sampling to determine soil characteristics (nutrient concentrations, hydraulic conductivity, texture, water retention) in the ~~irrigation laboratory as well as terrestrial laser scans of the AFS is no longer a~~ water but rather an energy limited system. ~~During field site, especially of the measurement~~ windbreaks. The continuous measurements covered meteorological, soil water content and soil water potential observations over a six-month period (in summer). These were applied to understand soil water dynamics during rainstorms and dry spells, including root water uptake as well as soil water storage. We recorded in total 13 rainfall events ~~were recorded~~ delivering 5.5 – 117.6 mm of rainfall with an intensity of 0.4 to 5.7 mm ~~hr~~h⁻¹. ~~Root water uptake and event analysis show~~ Further analyses showed that infiltration ~~to is~~ likely ~~occur via macro-pore~~ dominated by preferential flow, with root water uptake potentially occurring in two depth zones corresponding to different plant communities. ~~Soil~~ While soil water content varied by depth and was influenced by physical and environmental factors, ~~but~~ it was generally higher in the intercrop zone than within the windbreak influence zone. ~~Soil moisture~~ During dry spells, soil water content did not ~~fall~~ drop below the water content ~~at of~~ the permanent wilting point (~~←~~ (< -1500 kPa). Values corresponding to soil water tensions above 1000 kPa were recorded on several occasions, these were mitigated by irrigation, and thus, did not result in water stress. Nutrient distribution and soil physical properties differed near the windbreak in comparison to the blackberry crop and the carbon sequestration potential is great in comparison to monoculture farming.

~~The interdisciplinary work explored numerous aspects of AFS and acquired different perspectives, confirming hypotheses through cross method analyses.~~

45 **1-Introduction**

We could demonstrate positive effects of the windbreak on the water balance and dynamics in the blackberry field site, even though questions remain as to the extent of these benefits and how they compared to disadvantageous aspects brought about by the presence of the trees (e.g. increased water usage). Irrigation did, in fact, shift the AFS from a water-limited to an energy-limited system.

50 1 Introduction

In a changing ~~and challenging~~ world, agricultural flexibility and adaptation measures are required to ~~maintain~~uphold and enhance ~~the living standard of~~ global ~~citizens~~living standards, while ~~facilitating ecosystem protection~~protecting and ~~restoration~~restoring ecosystems, as well as ~~ensuring~~to ensure agricultural productivity ~~in the light of increasing frequency of~~ amid more frequent water shortages, particularly in the global south (Douville et al., 2021). ~~One~~A promising mitigation measure to address ~~the~~these pressing challenges ~~in the agricultural sector~~ is the reintegration and improvement of agroforestry systems (AFS). AFS ~~describes~~describe the combination of woody perennial species with crops and/or livestock ~~complements and enhances resilience and productivity of existing agricultural systems, provide new perspectives and~~components. It has the potential to deliver multiple benefits and offer new perspectives for existing agricultural systems including their greater resilience and productivity (Sheppard et al., 2020a). AFS can ~~be applied within~~modify existing agricultural land and take many temporal and spatial forms differing in both composition and arrangement, ~~examples~~. Examples of commonly practiced systems include: alley cropping (crops/plants are grown between rows of trees or shrubs), hedgerows and windbreaks, multi-strata agroforestry (multiple layered trees and crops), parklands, boundary planting and planted fallows (Kuyah et al., 2019). Benefits of incorporating woody perennials into agricultural systems encompass non-timber forest products, animal fodder and building materials, alongside increased household resilience (Kuyah et al., 2019; Sheppard et al., 2020a, b). Simultaneously, ~~such systems~~AFS promote a more sustainable and diversified land use (Mbow et al., 2014; Rosenstock et al., 2019; Wilson and Lovell, 2016; Jose, 2009) in contrast to conventional modern monocropping systems (~~Kuyah et al., 2019; Sheppard et al., 2020a~~)(Kuyah et al., 2019; Sheppard et al., 2020a). Multiple on-site environmental benefits include soil conservation, nitrogen fixation, nutrient input, improved water infiltration capacity, enhanced water quality, reduced evapotranspiration, reduced surface runoff and erosion, and stable soil fertility leading to sustainable agricultural land use (Mbow et al., 2014; Rosenstock et al., 2019).

Tree shelterbelts ~~such as~~and windbreaks have various impacts on the microclimate within their zone of influence, which in turn affect the water balance. The maximum zonal effect ~~extends~~may extend five times the height of the windbreak downwind and for a short distance upwind (Campi et al., 2009; McNaughton, 1988). The reduction of wind speed and shading influences evapotranspiration; as well as air temperature and promotes dew formation, while the ~~leaf area~~leaves and branches intercept rainfall. Dew formation is increased by up to 80 %, resulting in an increase of precipitation by up to 20 % and soil ~~moisture~~water content by up to 10 % (Nägeli, 1943; Van Eimern et al., 1964). Windbreaks have been found to reduce wind speed and potential evaporation on the leeward side by up to 70 % and 30 ~~%~~, respectively ~~on the leeward side~~ (Veste et al., 2020; Hintermaier-Erhard and Zech, 1997; Häckel, 1999). Such windbreak effects result in reduced wind erosion and consequently ~~a lesser~~less reduction in soil quality; the wind would otherwise transport the finest topsoil fractions (alongside any nutrients) away (Shi et al., 2018; Shao, 2008). Besides reducing erosion losses, windbreaks also improve nutrient cycling efficiency (Sileshi et al., 2020). Due to their small footprint, windbreaks may only contribute ~~only~~ moderately to direct carbon and nutrient enrichment, although the increased presence of woody biomass and ~~litterfall present increased benefit over that provided by a treeless landscape~~. related litterfall present provide a benefit compared to a treeless landscape (Sheppard et al., 2024). Indirectly, however, windbreaks can increase carbon storage and soil conservation through improved crop productivity (Albrecht and Kandji, 2003). ~~However, their~~In a comprehensive review on US windbreaks, Smith et al. (2021) found that the main drivers leading to windbreak removal are the poor conditions of the trees, the age of vegetation, conflicts with irrigation and machinery, and competition with crops. The first two points highlight the importance of proper windbreak maintenance, intrinsically coupled with additional time and labour. The latter two points demonstrate how important it is to design windbreaks appropriately, so that resource competition between tree and crop can be limited by e.g. suitable spacing and choice of species in combination. Within this concert however, the windbreak's effect on the local water balance remains a critical research challenge.

Water availability for plants is affected by many factors, ~~such as water supply from.~~ While precipitation (~~climate~~) and ~~and~~ potential evapotranspiration determine the climatic water supply and demand (Lal, 2020), the supply-demand ratio can substantially be altered by irrigation (~~management~~). The most important terrain characteristics, ~~are~~ land use, ~~specific soil properties and evapotranspiration potential (Lal, 2020).~~ soil infiltration and soil water holding properties. Soil texture, organic matter content, and aggregation state are important factors controlling soil hydraulic parameters, ~~along with~~ alongside climatic and vegetation factors. ~~The water content extracted from the~~ Soil water retention curves characterise the strength of capillary forces acting on soil water, and are thus, useful to assess both its binding status and availability to plants, especially in water-limited regions. While the corresponding soil water content at field capacity (FC) ~~determines the point at which the soil holds as much~~ maximum water ~~as possible~~ storage against gravity) ~~and at,~~ the water content at tensions less than the permanent wilting point (PWP; ~~the minimum amount of soil water required that a~~ ≈ -1500 kPa) is not plant ~~does not wilt without recovery)~~ provides an estimation available anymore. The effective field capacity, i.e. the difference of both values, can be interpreted as the plant-available water in the pore space. ~~Especially~~ stock. Note that, especially around FC, small fluctuations in matric potential amount to large ~~variation~~ variations in water content due to the steep slope of the water content curve ~~around the FC.~~ For this reason, ~~water retention curves can be a useful tool to assess the water status and availability, especially in water-limited regions.~~

Our rationale is to explore the “promise” of AFS of an improved water and nutrient status, using an established irrigated AFS combining alder as a linear windbreak with a blackberry crop as a benchmark system. South Africa, particularly the Western Cape region, is a water-scarce region facing severe challenges in sustaining agricultural productivity in the future due to projected increases in air temperature and longer dry spells as a consequence of climate change (e.g. Fauchereau et al., 2003). The high wind speeds along the coastal region result in high potential evapotranspiration (PET) ~~),~~ and thus, a strong atmospheric demand. The steady-state connection between the potential (PET) and the actual evapotranspiration (AET) can be assessed with the Budyko framework, ~~which is widely used for hydro climatic classification in hydrology. It (Budyko, 1974).~~ This relates the annual-actual to potential evapotranspiration and (release over demand) to the dryness index (precipitation supply over potential evaporation demand). The Budyko curve is often used to characterise the long-term average water and energy balance ~~on a~~ catchment or regional scales ~~(Budyko, 1974),~~ and can therefore, be used to categorise areas into different climate regimes, namely:

- 1) Energy limited settings with an aridity index (precipitation / ~~potential evapotranspiration~~) > 1 and $PET > 1$. More water could evaporate, if more energy were available. AET is limited by the radiative energy supply (AET = PET).
- 2) Water limited settings with the aridity index < 1 . ET is limited by the water supply (AET < PET).

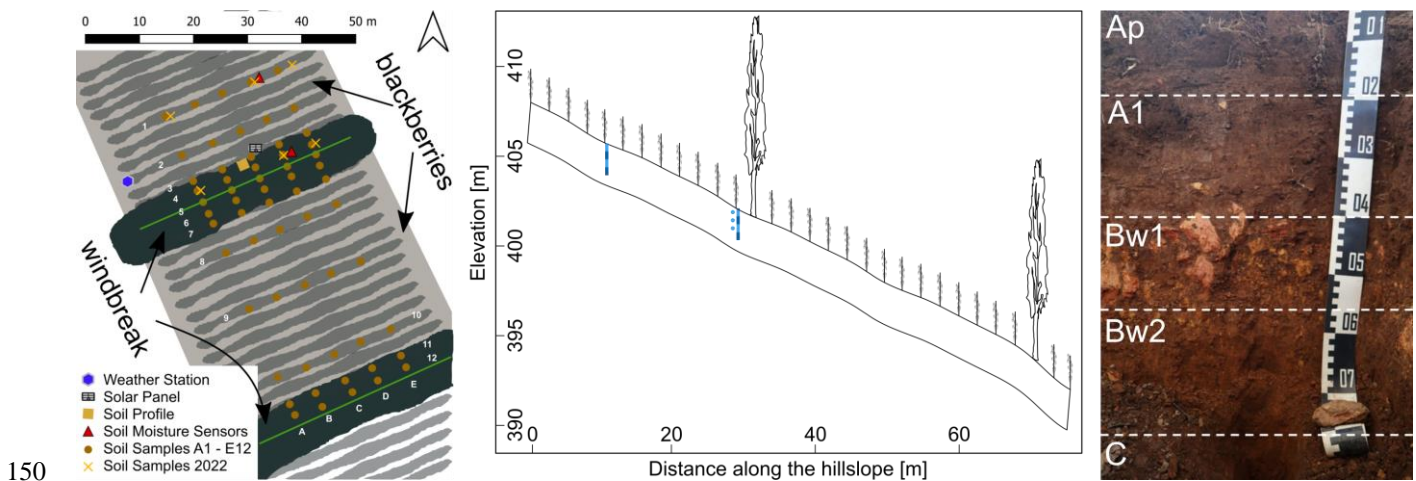
Windbreaks carry the potential to reduce the necessary water ~~input demand (supply by precipitation, and irrigation),~~ ensuring sufficient water availability for crop plant growth. However, field and simulation studies investigating system-level feedbacks between trees, crops and microclimate are lacking, especially for drylands (Sheppard et al., 2020a). For this reason we tested whether a multidisciplinary and multi-method approach to characterise an established irrigated fruit orchard in South Africa is able to close this gap and deliver a holistic system perspective on the processes affecting water availability and fluxes. Specifically, we combined various campaign-based measurements from multiple disciplines with high-frequency, long-term monitoring of water and energy balance components to capture both spatial variability and temporal dynamics. We used terrestrial laser scanning (TLS) ~~technology~~ as a novel method for investigating three-dimensional structures of trees and their shade patterns (Bohn Reckziegel et al., 2021; Raunonen et al., 2013). We took undisturbed soil samples to analyse soil physical properties, such as the site-specific water retention curve and soil hydraulic conductivity, which are key to determine the plant-available soil water storage. Transects of surface soil samples were analysed to assess the influence of the windbreak on nutrient distribution. The long-term monitoring included high-frequency soil ~~moisture~~ water content and soil water potential to provide information on temporal dynamics of potential water limitation for transpiration. This was combined with meteorological records of precipitation, solar radiation, air temperature, relative humidity and wind speed, thus, allowing for

135 the characterisation of both water supply and potential evaporation demand and the related energy limitation. By merging the different methods we could infer process such as infiltration through the combination of nutrient analyses with soil water dynamics during rain events, or by reflecting on the energy budget through shade-cast simulations and evapotranspiration estimates. The main objective of this study is was to synthesizesynthesise dominant controls on water availability from these observations and to particularly evaluate the positive and negative effects of the windbreak on the water and nutrient balance and cycling in the AFS. ~~We also reflect on the feasibility of our multidisciplinary approach to characterise AFS in data scarce regions.~~

2 Materials and methods

2.1 Site description

145 The field site is located in the Western Cape Province, South Africa, nearclose to the city of Stellenbosch on a fruit orchard located on the southern flank of the Simonsberg (fig. 1). It is situated1 on a 30 % slope at an elevation of approximately 400 m above sea level. The region is dominated by a Mediterranean climate with hot, dry summers (Dec-Mar) and mild, moist winters (May-Sep) (Ndebele et al., 2020). Mean annual precipitation sum in Stellenbosch is 742 mm (Meadows, 2015). The regional wind system includes strong winds from the southeast that dominate the summer months.



150 Figure 1. Left: SamplingSketch of sampling design and location of the alder-blackberry AFS near Stellenbosch, South Africa. For illustrative purposes, the alder canopy is shown in green and the blackberry rows in grey shading. The triangles show the location of the soil water sensors for the monitoring, each point signifying four soil moisturewater content sensors and three matric potential at the point near the windbreak. Middle: Transect of the slope indicating the location of soil moisturewater content sensor stacks in-theat different depths (blue squaresrectangles) and matric potential sensors (blue circles). Right: Photograph of the soil profile with horizon delineations and characterisation as dystric cambisol (loamic, colluvic, humic).

160 The study site contains multiple single tree row windbreaks of Italian alder (*Alnus cordata* (Loisel.) Duby)), a non-native deciduous tree species establishedplanted perpendicular to the prevailing wind direction i.e.. The 40 study trees are arranged in a linear form from east-northeast to west-southwest. The with regular between tree spacing, the studied windbreak has a length isof 45 m and the 40 trees are planted in a regular spacing (fig. 1). The windbreak trees developed a particular oval crown shape due to the close within row spacing of the windbreak with exceptionexception of the last trees in the row, which developed a rounded crown on the row edge. The trees are approximately 15 to 20 years old and are pruned annually to limit encroachment on the first rows of the intercropping space. The study windbreaks were spaced approximately 40 metresm apart were-situated-withinwith blackberry (*Rubus fruticosus* L. ‘Var Waldo’) fields-with-blackberry canes arranged in parallel rows 2 m apart and perpendicular to the slope between each windbreak row. The 5-6 year old blackberries usually start shooting in late spring (October) and are harvested from mid-January to mid-March. One month after fruiting, they are cut back to the

base. In the summer months (late November to January) a drip system ~~provides~~provided irrigation. ~~Approximately~~Informally, ~~approximately~~ three days a week, each plant ~~is~~was irrigated with 2.3 L d⁻¹, distributed in cycles of 10 ~~minutes~~min. Once a year, before spring, a slow-release fertiliser ~~is~~was applied.

2.2 Field measurements, sampling, monitoring and laboratory analyses

A field campaign was conducted in September 2019 where the majority of the one-time sampling and on site measurements ~~on-site~~ were carried out. During this campaign, the long-term monitoring equipment for water fluxes was also installed ~~which~~ ~~measured, actively recording data~~ between September 2019 and March 2020 (hereafter called the measurement period). An additional small scale campaign took place in March 2022 ~~where, when~~ further undisturbed soil samples were taken.

2.2.1 Meteorological measurements

Meteorological data were recorded in 10 ~~minute~~ min intervals from mid-September 2019 until mid-March 2020 with an ATMOS 41 weather station (METER Group) in combination with a ZL6 Cloud90 data logger. Figure 1 shows the position of the weather station at the study site. The following variables were measured at ~~two metres in a~~ height, ~~namely of 2 m~~: Solar radiation, precipitation, water vapour pressure, air temperature, barometric pressure, horizontal wind speed and wind direction.

2.2.2 Soil sampling and laboratory analyses

During the campaign in September 2019, a representative soil profile pit at the research site was prepared and described with field methods following the FAO guidelines for soil description (Jahn et al., 2006). A composite sample from each identified horizon was taken for soil texture and nutrient analyses in order to classify the soil according to the World Reference Base for Soil Resources, WRB (IUSS Working, 2014) (fig. 1). Spatial topsoil (0-5 cm) sampling was carried out along five parallel downslope transects, crossing several blackberry and two alder rows (fig. 1). Per transect, 12 samples of approximately 300 g were liberated with a hand shovel, yielding a total of 60 topsoil samples. These samples were air-dried and passed through a 2 mm sieve, before transporting them to Germany for physical and chemical analyses.

From each soil sample, an aliquot was dried at 105 °C to determine residual water content. Subsequently, the samples were milled (Siebtechnik TEMA), dried again at 105 °C, and combusted at 1150 °C for total carbon (C) and nitrogen (N) concentrations (Vario EL cube, Elementar Analysensysteme GmbH, Langensfeld, Germany). For soil classification purposes, some laboratory analyses with air-dried soil samples were carried out. We determined pH in a 1:2 soil-solution-ratio with ultra-pure water and with a glass electrode (pH meter 704, METROHM GmbH, Filderstadt). Potential cation exchange capacity (CEC_{pot}) was determined using 1M ammonium acetate at pH 7. Exchangeable cations (Ca, Mg, K, and Na) were displaced with sodium acetate and measured through ICP-OE spectroscopy (Spectro Ciros CCD ICP Side- on Plasma Optical Emission Spectrometer, Kleve, Germany). Soil texture of the soil profile samples was conducted after removal of organic material with H₂O₂ (hydrogen peroxide (H₂O₂) and chemical dispersion with tetrasodium pyrophosphate (Na₄P₂O₇) according to the sieve and pipette method (ISO 11277:2002).

Additionally, we took three undisturbed soil samples in 250 ml cylinders from a selected soil profile, pit, one at the surface and one each at depths of 0.3 and 0.5 m during the field campaign in September 2019 to determine soil hydraulic properties and some additional variables. Soil hydraulic conductivity of the undisturbed samples was measured with the Ksat apparatus (UMS GmbH, Munich). Soil water retention characteristics on drying samples were measured on the same samples in the HYPROP device (UMS GmbH, München, Germany). A small fraction of the sample (about 10 g) was then transferred to the WP4C potentiometer (Decagon Devices Inc., Pullman, WA, USA) and subsequent weighing, further drying and measuring contributed further reference points to the water retention curve. Soil texture was determined through wet sieving of ground soil and smaller fractions were again separated with the sedimentation method after Köhn (ISO 11277:2002). Organic compounds were destroyed with the application of H₂O₂. ~~Soil hydraulic conductivity of the undisturbed samples was measured~~

210 ~~with the Ksat apparatus (UMS GmbH, Munich). The method is based on the Darcy equation, describing a flux through a saturated porous medium as product of the driving head difference and the saturated soil hydraulic conductivity. The device records the falling head of the water supply through a highly sensitive pressure transducer, which is used to calculate the flux. Soil water retention characteristics on drying samples were measured on the same samples in the HYPROP device (UMS GmbH, München, Germany). It records total mass and matric head in two depths in the sample over time while it is exposed to free evaporation. A small fraction of the sample (about 10 g) was then transferred to the WP4C potentiometer (Decagon~~
215 ~~Devices Inc., Pullman, WA, USA), where soil water potential was measured based on a chilled mirror approach. Subsequent weighing, further drying and measuring contributed further reference points to the water retention curve.~~

In the second ~~small~~ campaign in March 2022, 12 additional undisturbed soil samples were taken and analysed in the same way as described above. We took the samples in ~~blackberry row 1~~ the first (within the alder root zones) and ~~8~~ eight (as a reference without the windbreak influence) blackberry row at three positions (east, mid and west). At each position we sampled at two
220 depths, as close as possible to the surface and at 20 cm depth.

2.2.3 Monitoring ~~of~~ soil water dynamics

Eight TDR probes (Trime Pico IPH, IMKO GmbH, Ettlingen, Germany) were installed in two 4.2 cm diameter access tubes. Four sensors per tube were assembled stacked directly on top of each other. The individual sensors have a length of about 0.18 m, integrating over this depth, so four sensors per tube covered a depth of approximately 0.8 m. ~~The lateral penetration depth of the microwave impulse of 5.5 cm yields an integration~~ Each sensor has a measurement volume of ~~approximately 3 L per sensor~~ 1 dm³. The sensors were installed at two locations (fig. 1): 1) In the first blackberry row of the field, close to the windbreak, within the assumed rooting influence of the windbreak. 2) In ~~row 8 of the eighth~~ row 8 of the eighth blackberry ~~field row~~, as a control ~~site~~ removed from the rooting influence of the windbreak. Two additional TDR probes (Trime PICO32, IMKO GmbH, Ettlingen, Germany) with a measurement support volume of approximately 0.25 L were installed at a depth of 0.1 m next to
230 each tube, to ~~cover~~ explicitly cover the topsoil ~~moisture~~ water content. Furthermore, we inserted three dielectric water potential sensors (MPS-2, Decagon Devices, Inc., Pullman, WA, USA) in a profile adjacent to the windbreak tube at depths of 0.1, 0.3 and 0.4 m to measure matric potential.

Data were recorded at 15-minute min intervals (TrueLog100, TRUEBNER GmbH, Neustadt, Germany) between 21 September 2019 and 14 March 2020 ~~and retrieved data were checked for obvious outliers e.g.,~~
235 ~~due to maintenance work and other technical disturbances. For most analyses, data were aggregated to averaged hourly data.~~

2.2.4 Terrestrial laser scanning and windbreak characteristics

The research site was digitised/scanned with a terrestrial LiDAR in September 2019 under negligible wind conditions. A ~~Rieg~~ RIEGL VZ 2000i (RIEGL Laser Measurement Systems GmbH; Horn, Austria) was employed with a multiple-scan position approach to ensure a three-dimensional representation of the target vegetation and to ~~reduce the~~ occlusion effects
240 (Wilkes et al., 2017). As an amalgamated scanning target, the central windbreak was scanned from 32 scanning positions covering the alder trees; 14 positions were within 10 m distance from the windbreak, and up to 10 m away from each other. The remaining 18 positions were located at a distance of 15 to 25 m away, with wider scanning step distances between scans. Trees were scanned under leaf-off conditions, however a few trees had retained dried leaves ~~on~~ within the inner crown from the previous vegetation season.

245 ~~Values of diameter at breast height (DBH, measured at 1.3 m) were measured manually in March 2020 and March 2022, for 17 trees within the windbreak row (eight trees left and right of the sensors with the central tree being closest to the sensors).~~

2.3 Data analyses

2.3.1 Meteorological data processing

250 The ultrasonic anemometer recorded unusually high values during heavy precipitation events. This error also occurred in some cases in the morning, likely ~~attributed~~attributable to ~~dew formation-water on the sensor affecting the transmission of the ultrasonic electromagnetic reflection~~. All events in question were referenced to the Stellenbosch airport climate station ~~wind~~. Wind and gust speed were considered outliers and replaced with NA if their values seemed unreasonable. The decision process was straightforward, as most of the outliers reached the maximum measurable wind speed of 30 m s⁻¹ on low wind days. The integrated cloud service was used to calculate ~~potential evapotranspiration (PET)~~PET by using the FAO Penman-Monteith

255 method (Allen et al., 1998) based on the observations and yielded daily values.

The aridity index (PET/P) was calculated ~~based on~~after Budyko (1974) for a) the whole observation period and b) the same period, but with an addition of 20 mm d⁻¹ on three weekdays to account for irrigation inputs between December and March on days without precipitation.

260 Precipitation events were identified by an automated detection routine, which defined a precipitation amount of > 2 mm in less than six hours as a unique precipitation event and extracted start time and duration, precipitation amount and precipitation rate for each event. Precipitation events < 2 mm in six hours did not result in significant changes in topsoil ~~moisture~~water content, and were therefore not considered in further analyses.

2.3.2 Soil sample analyses

265 The nitrogen and carbon concentrations of the soil transect samples were considered replicates per row. Therefore, all five transect samples of one row were averaged to obtain a more robust estimate of the overall concentration distribution across the slope. The water retention curves of the profile soil samples were parameterised with the PDI model (Peters, 2014), which is a modified version of the work from Van Genuchten (1980) and Mualem (1976) and used to estimate plant-available water as the difference in volumetric water content between FC and PWP.

2.3.3 Evaluation of soil water dynamics from the monitoring data

270 ~~The volumetric water content time series were used to retrieve information on root water uptake based on Guderle and Hildebrandt (2015) and changes in soil water storage during precipitation events. Daily root water uptake (RWU) was estimated from hourly water content time series with the Python package introduced by~~The retrieved data were checked for obvious outliers e.g. due to maintenance work and other technical disturbances. For most analyses, data were aggregated to averaged hourly data. ~~Jackisch et al. (2020). The algorithm derives RWU from stepwise diurnal changes in soil moisture~~

275 ~~between two consecutive days. RWU is assumed to be the decrease in soil moisture over the course of a day i.e. between two nights. For each water content sensor, daily soil moisture was checked and if it contained a stepwise decrease, RWU was calculated for that day as the difference in absolute soil moisture values between two nights including a nocturnal correction. If no decrease was found, RWU was not calculated and the window moved to the next day. The evaporative fraction was calculated as the ratio between actual and potential transpiration with the assumption that AET is represented by RWU.~~

280 After general inspection of the time series and comparison with one another, the volumetric water content time series were used to retrieve information on root water uptake (Guderle and Hildebrandt, 2015) and on changes in soil water storage during precipitation events. Daily root water uptake (RWU) is derived after Jackisch et al. (2020) including a nocturnal correction from stepwise diurnal changes in soil water content between two consecutive days assuming that RWU is the decrease in soil water content between two subsequent nights. If the hourly soil water content time series of a sensor did not show a stepwise

285 decrease, RWU could not be calculated for that sensor on that day. The water limitation factor f_w (e.g. Ghausi et al., 2023) was calculated as the ratio between actual and potential transpiration with the assumption that AET is represented by RWU.

We determined soil water storage changes by subtracting two successive soil ~~moisture~~water content values and by multiplying by the sensor depth increment of 0.18 m. ~~These changes were used~~This allows to compare storage changes between windbreak-influenced and reference ~~sites~~location at the different depths and to optionally close the water balance during precipitation events.

2.3.4 Tree and windbreak characteristics

The point clouds derived from the TLS campaign were processed to obtain structural tree data, foliage data, and windbreak characteristics. Co-registration of scan positions was carried out using the software RiSCAN PRO 2.11.3 (RIEGL Laser Measurement Systems GmbH; Horn, Austria), following standard software protocol to generate project point clouds. In the single-scans, points were removed if the distance was further than 60 m from the scanning position; or the pulse deviation was greater than 10, and with calibrated reflectance lower than -10 dB and greater than 0 dB. Additionally, isolated scan points were removed as these were considered to be noise. Lastly, cubic down-sampling (25 mm voxel side) was applied to the final project point cloud.

The point cloud model of the windbreak was extracted and individual tree point clouds were manually segmented for 18 individuals in sequence, starting from one of the edges. ~~Tree~~The tree point clouds were used to model the tree structures and estimate tree parameters (e.g. diameter at breast height, 1.3 m from ground, tree height and volume) with TreeQSM v2.3.2 (Calders et al., 2015; Raunonen et al., 2013; Raunonen, 2017). ~~After visual inspection, tree point clouds were categorized into occlusion classes with the goal of efficiently estimating~~An estimation of the uncertainty of the tree parameters derived from the quantitative structure models (QSM). ~~For this optimisation process, one tree in each occlusion category~~ was ~~randomly chosen and~~carried out by categorising the tree point clouds into occlusion classes, the estimated precision of one randomly chosen tree was extended to all individuals in the group (Raunonen, 2017). Wood volume was converted to woody biomass by assuming a wood density of 420 kg m⁻³, considering an average value for *Alnus sp.* (after: Worldwide 'open access' tree functional attributes and ecological database, Harja 2023). The belowground root biomass was estimated as 28.54 % of the aboveground woody biomass (Frouz et al., 2015).

The leaf creation algorithm by Bohn Reckziegel et al. (2022) was used to estimate foliage by restricting leaf classes to “small”, “medium” and “large” categories with corrected ratios according to leaf sizes for *Alnus sp.* (San-Miguel-Ayanz et al., 2016). The leaf spacing definition was varied from 2.0 to 3.0 cm to estimate total leaf area on a tree basis and leaf dry mass assuming the specific leaf mass of black alder (*Alnus glutinosa* (L.) Gaertn.) of 13.3 ± 0.3 m² kg⁻¹ (Johansson, 1999). The calculated leaf area index (LAI) was used to approximate cumulated interception over the course of a rain event. An empirical estimation of a leaf area dependent interception storage value of 0.0001 m was applied, as such a value has been used in many different modelling studies providing satisfactory estimates of the interception storage (e.g. Zehe et al. (2001)). The leaf area dependent interception storage value is multiplied with the LAI to yield interception estimations.

The shadow model by Bohn Reckziegel et al. (2021) was utilised to estimate shading effects of the windbreak through the QSMs. This enabled an estimate of the shade cast under and surrounding the leafless windbreak ~~under leaf off conditions~~. A nominal date representing the site conditions was chosen as 25 September as experienced in the field campaign. The initially acquired QSMs were simplified with two replacement iterations (Bohn Reckziegel et al., 2022). The tree structures were bound together in a data frame to expand the model capabilities from single- to multiple-trees in a simulation. After removing four trees closest to the windbreak edge, we mirrored the ~~retained~~remaining trees for simulating a windbreak ~~session~~ with a total of ~~2629~~ trees. The shadow model was fed with ~~minute~~60 second solar irradiance data from 2019 (January to December) provided by Stellenbosch University (~~Stellenbosch Weather~~)(Stellenbosch Weather, 2023) and derived from the Sonbesie meteorological station (33°55'42.84" S, 18°51'55.08" E, 119 m a.s.l.) less than 10 km from the research ~~location and~~ shadow site. Shadow projections were simulated on a ground surface of 0.4 ha (100 m East-West, 40 m North-South) with a

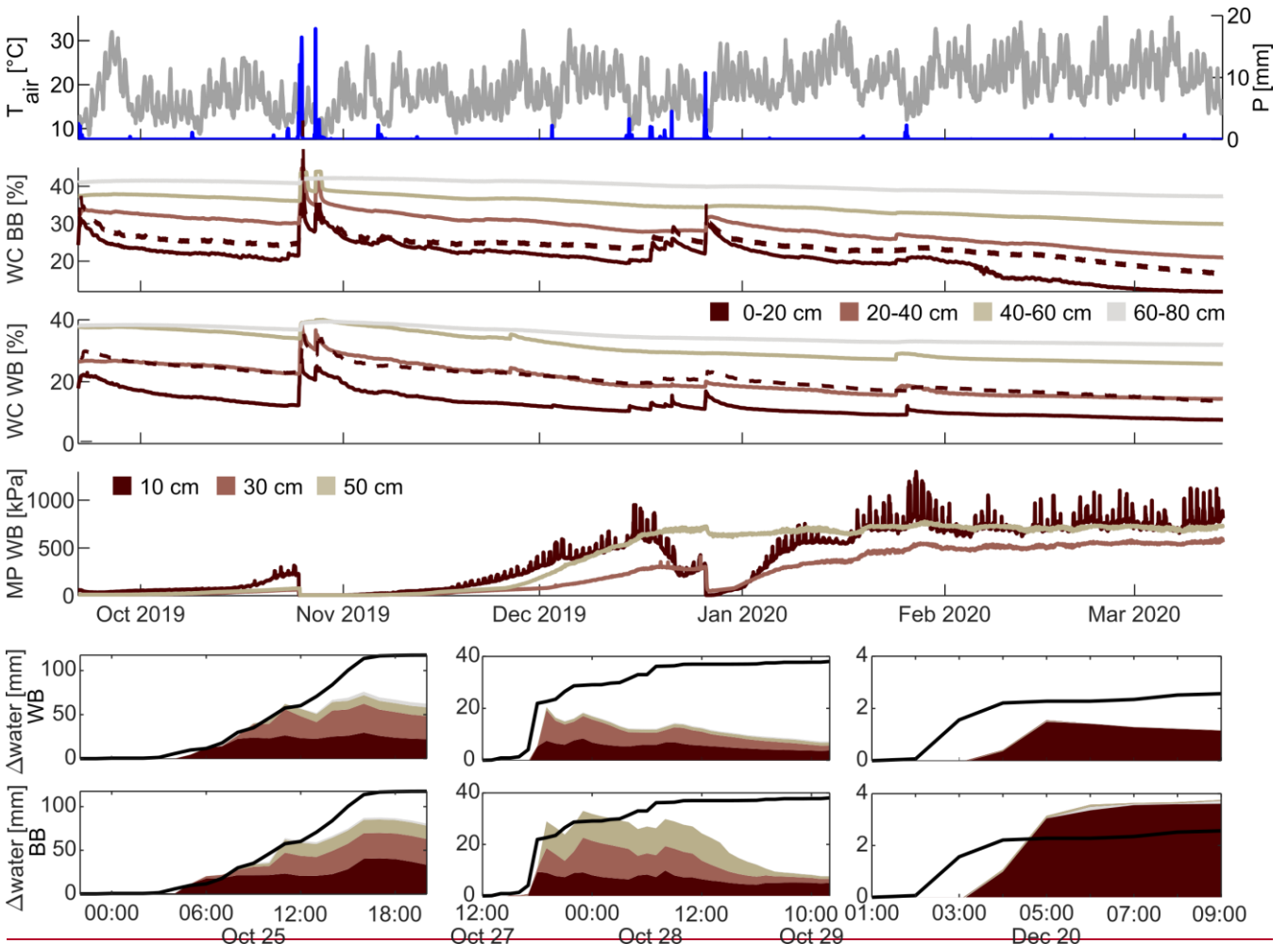
grid cell size of 10 cm x 10 cm, and centralised to the windbreak position for each time interval of 10 ~~minutes~~min, ~~this was~~
~~applied in order to simulate the shade cast specific to the windbreak in its defined position.~~

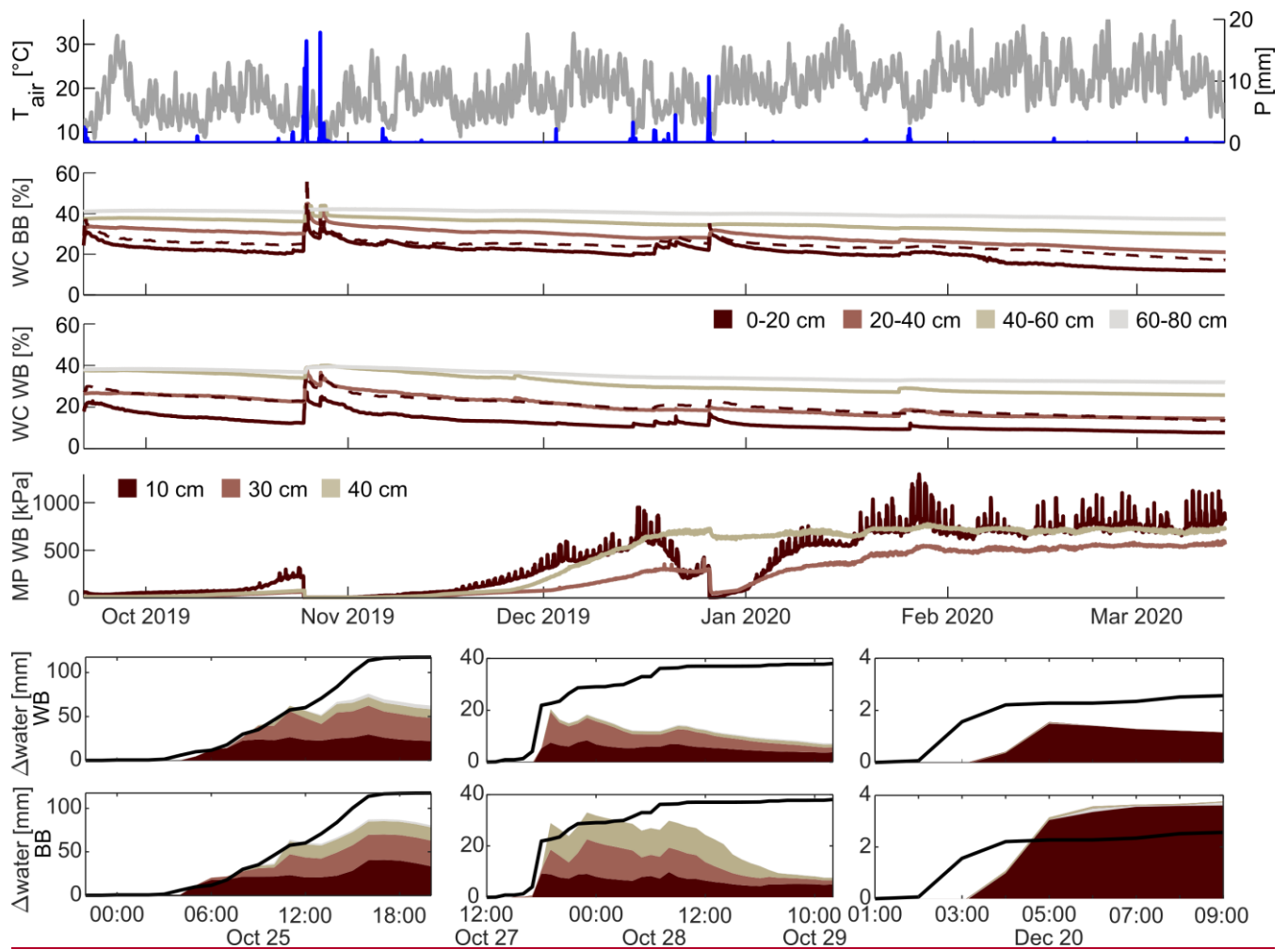
330 Measured DBH values were used to estimate the biomass gain over the course of a year, which in turn can reveal information
on the alders' water use efficiency (WUE). The biomass for both days for different tree compartments (total aboveground and
root) was estimated using the equation given Gholz et al. (1979) for red alder (*Alnus rubra* (Bong.)) as a proxy for *A. cordata*.
The WUE is then calculated by dividing the difference in total biomass (sum of both compartments) of each year by the annual
335 transpiration (1150 mm yr⁻¹ observed by Veste et al. (2020) in 2015-2016 on a nearby vineyard). Multiplying this by the actual
biomass produced based on the TLS derived parameters gives a rough idea of water usage of the alder during its lifetime (under
the strong assumption that WUE is constant throughout a tree's lifetime).

3 Results

3.1 Meteorological observations

The measurement period falls within the South African summer months. The average measured air temperature was 19.5 °C
340 with a minimum of 7.5 °C and a maximum ~~value~~ of 35.7 °C. ~~A total of 245 mm of~~The precipitation ~~fell~~sum during the
measurement period totalled 245 mm, notably, 118 mm fell during one single storm event on 25 October 2019 (fig. 2, upper
part). The measured wind direction ~~within~~at the study site was predominantly westerly in spring/early summer and easterly in
late summer/autumn. ~~Mean wind with an average~~ speed ~~was of~~ 2.2 m s⁻¹ ~~and reached maximum speeds of > 30 m s⁻¹ on two~~
~~occasions~~. PET was estimated to average 5.2 mm d⁻¹, with a peak in late February of 11.2 mm d⁻¹ (data not shown) and
345 cumulative PET reached a total of 913 mm for this period.





350 Figure 2. Meteorological observations (precipitation P, air temperature T) of the whole measurement period (upper panel). Soil moisture (volumetric water content (volumetric WC) and matric potential (MP) time series at both locations (middle panels; WB: windbreak, BB: blackberries). The dashed line represents the 10 cm soil moisture sensor. The lower panels show cumulative precipitation (line) and cumulative soil water storage change of each sensor for selected precipitation events, (see fig. A1 for remaining events), for both the windbreak (upper row) and the blackberry (lower row) location. The different colours represent the different depths of the sensors.

The aridity index for the entire period was calculated to be 3.7, and with gave a value of 3.7, clearly larger than 1, fall into the water limited/arid region of the Budyko curve. When accounting for the additional irrigation in the summer the aridity index dropped to 0.65, indicating a humid/energy limited regime.

360 Thirteen precipitation We identified 13 rainfall events > 2 mm were identified, ranging in total precipitation from 2.5 mm to 117.6 mm and in measured maximum intensity from 4.1 to 82.6 mm h⁻¹ (table 1). On average most of the events had a precipitation rate of 1.6 mm h⁻¹, therefore, considered low intensity events with mean durations of 1.6 mm h⁻¹ and a duration of 11 h 41 min. The longest event lasted 37 h.

365 Table 1. Observation data extracted for the Observed precipitation (P) events above 2 mm per 6 hours (Ini = initial) h.

Event	Start date	Duration [hh]	P. Amount [mm]	Max. P. Rate [mm h ⁻¹]	Ini-Initial Soil Moist. [-]
1	21 Sep 2019 11:00:00	23.0	10.5	12.2	0.51
2	08 Oct 2019 20:00:00	2.0	2.5	7.1	0.51
3	23 Oct 2019 11:00:00	6.0	4.1	22.4	0.37

4	24 Oct 2019 23:00:00	21.0	117.6	65.3	0.37
5	27 Oct 2019 13:00:00	37.0	38.1	82.6	0.59
6	06 Nov 2019 07:00:00	14.0	5.5	17.3	0.57
7	02 Dec 2019 21:00:00	3.0	2.6	9.2	0.32
8	14 Dec 2019 17:00:00	2.0	4.3	5.1	0.26
9	17 Dec 2019 17:00:00	15.0	8.5	72.4	0.26
10	20 Dec 2019 02:00:00	7.0	2.6	4.1	0.28
11	21 Dec 2019 05:00:00	1.0	4.6	10.2	0.30
12	26 Dec 2019 06:00:00	10.0	23.1	45.9	0.32
13	25 Jan 2020 21:00:00	11.0	7.1	13.3	0.24

3.2 Soil Sample analyses

3.2.1 Soil profile and undisturbed samples

370 The soil profile (fig. 1) was classified as Eutric Cambisol (Colluvic, Humic, Silty) based on the international soil classification system WRB. ~~It exhibits a silty~~The texture is silty across all horizons (table 2) with a high base saturation and an accumulation of colluvial material eroded from upper parts of the slope in the shallower part of the profile. The supplementary qualifier “humic” (~~IUSS Working, 2014~~)(IUSS Working Group, 2014) was added due to the high average carbon content within 50 cm from the mineral soil surface.

375 Table 2. Characteristics of the five horizons identified in the soil profile (fig. 1).

Horizon	Depth	Texture	pH (H ₂ O)	CEC [mmol _c kg ⁻¹]	Base saturation [%]	C(org) [%]	N [%]
Ap	0-20 cm	Silty Clay Loam	6.9	221	74	2.89	0.17
A1	20-40 cm	Silty Clay Loam	5.8	175	28	2.37	0.13
Bw1	40-55 cm	Clay Loam	5.0	144	20	1.22	0.08
Bw2	55-75 cm	Clay Loam	4.9	127	24	0.89	0.06
C	> 75 cm	Clay Loam	4.8	117	26	0.54	0.05

380 The three undisturbed profile samples taken adjacent to the soil water equipment and the additional samples collected in 2022 were analysed for soil hydraulic properties (~~table 3~~). ~~The bulk density is overall moderate ranging from 1.01 to 1.25 g cm⁻³ except for the deepest profile sample of 1.49 g m⁻³. In the upper samples bulk density is greater at the windbreak, hence porosity and hydraulic conductivity smaller compared to the samples in the blackberry crop. (fig. 3, table A2).~~ The lower soil was homogeneous between locations. The topsoil was denser at the windbreak than at the blackberry and the overall moderate bulk density ranged from 1.01 to 1.25 g cm⁻³ with the exception of the soil profile sample at 0.5 m of 1.49 g m⁻³. Topsoil organic matter content was similar at both locations and decreased with depth (averages from 11.5 % in the shallow to 10.4 % in the deeper soil). The windbreak topsoil averages matched with the deeper soil averages for the following parameters (averages in parentheses): porosity (0.57, fig. 3), water content at FC (0.359 m³ m⁻³, fig. 3), PWP (0.171 m³ m⁻³) and PAW (0.187 m³ m⁻³). The blackberry topsoil had a greater porosity and the water content at FC and PWP as well as the PAW were lower. Topsoil hydraulic conductivity was nearly three times greater at the blackberry crop than at the windbreak, but only 20 % more in the lower soil depths (fig. 3).

385

390 ~~Table 3. Laboratory analysis of three soil samples taken adjacently to the soil moisture monitoring point near the windbreak at different depths. Abbreviations are: WB P – profile, WB – windbreak, BB – blackberries, E – east, M – middle, W – west, FC – field capacity, PWP – permanent wilting point, PAW – Plant available water. The values of the three columns from the right are estimated using the PDI water retention model (Peters, 2014). The last four rows are averages of the windbreak and berry location at the two depths.~~

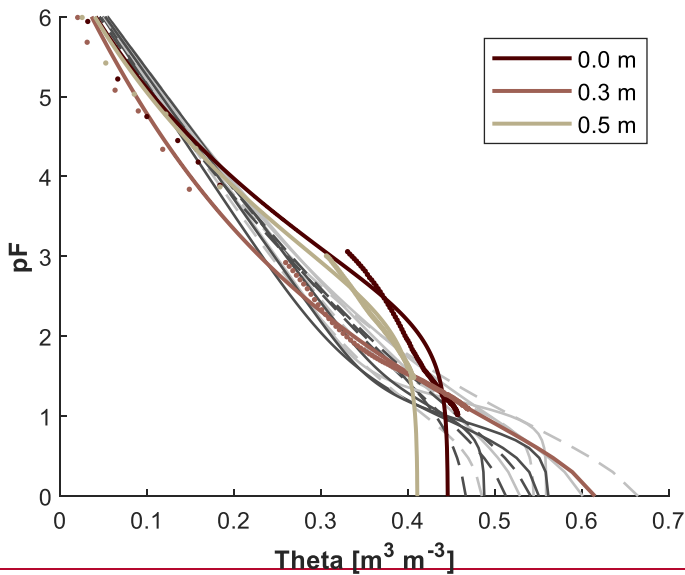
Location	Sample	Hydraulic	Organic	Bulk-density	Porosity	Wat.-Cont.	Wat.-Cont.	PAW
	Depth	conductivity (Ksat)	matter			FC	PWP	
	[m]	[mm hr ⁻¹]	[%]	[g cm ⁻³]		[m ³ m ⁻³]	[m ³ m ⁻³]	[m ³ m ⁻³]
WB P	0.0	263.1	15.1	1.17	0.56	0.426	0.178	0.248
WB P	0.3	108.7	9.3	1.11	0.58	0.367	0.136	0.231
WB P	0.5	3.2	7.3	1.49	0.44	0.393	0.169	0.224
WB E	0.05	203.3	6.6	1.19	0.55	0.368	0.165	0.203
WB E	0.28	94.05	10.2	1.16	0.56	0.396	0.168	0.228
WB M	0.05	114.5	13.9	1.19	0.55	0.364	0.174	0.191
WB M	0.26	111.4	10.3	1.18	0.55	0.335	0.164	0.172
WB W	0.05	171.9	14.2	1.19	0.55	0.373	0.175	0.199
WB W	0.23	426.6	11.5	1.12	0.58	0.358	0.179	0.179
BB E	0.10	688.8	11.9	1.01	0.62	0.322	0.158	0.164
BB E	0.25	186.8	11.5	1.25	0.53	0.379	0.180	0.199
BB M	0.10	255.7	12.7	1.06	0.6	0.327	0.169	0.158
BB M	0.25	189.3	6.9	1.21	0.54	0.393	0.176	0.216
BB W	0.10	379.8	9.7	1.13	0.57	0.346	0.178	0.168
BB W	0.25	413.1	12.0	1.04	0.61	0.331	0.170	0.161
WB	0.05	163.2	11.6	1.19	0.55	0.369	0.171	0.197
WB	0.25	210.7	10.7	1.15	0.56	0.363	0.170	0.193
BB	0.05	441.4	11.4	1.07	0.60	0.332	0.168	0.164
BB	0.25	263.1	10.1	1.16	0.56	0.368	0.175	0.192

395 ~~In contrast, in the lower samples this is not observable and the parameters are rather similar with the exception of saturated hydraulic conductivity. This was seen to be slightly greater within the windbreak, here, saturated hydraulic conductivity is greatest in the shallower samples and decreases with depth, whereas within the blackberry crop it is slightly greater in the lower samples.~~

400 ~~The organic matter content varies between 6.9 and 15.1 % (table 3) across the samples, but no clear pattern shows between the averages of the locations (11.05 ± 0.1 %). The shallower samples have larger organic matter content, which decreases with depth.~~

The soil water retention curves (fig. 3) of the top and bottom sample exhibit similar shapes but different porosities, whereas the middle sample curve is less steep and decreases more homogeneously starting at a much higher saturated water content.

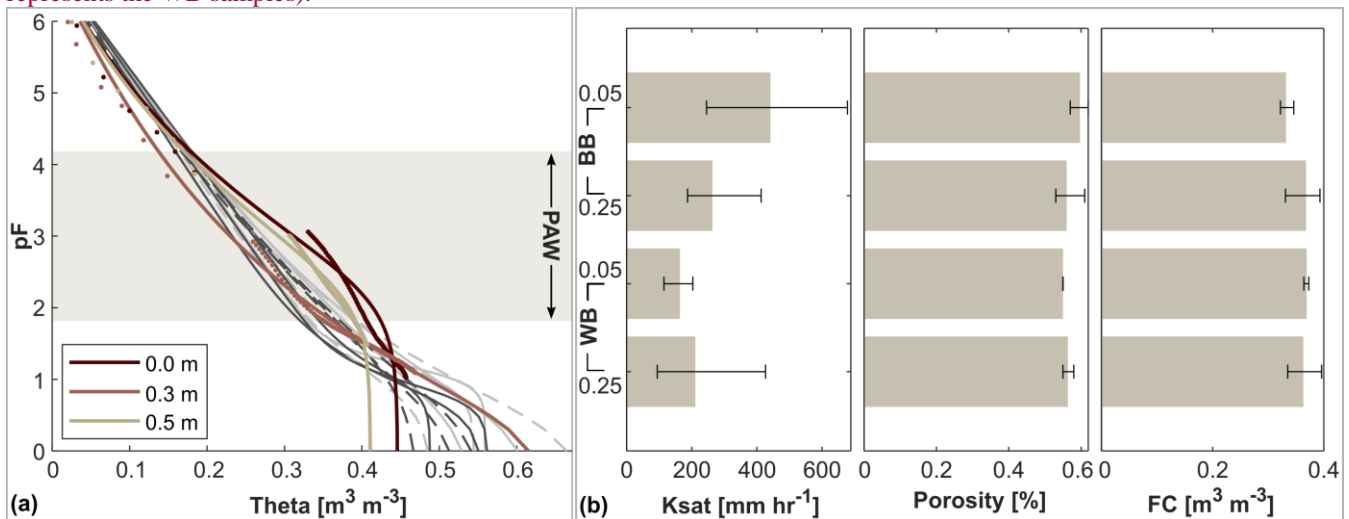
405 The deepest sample has the lowest saturated water content and a porosity of 0.44, while the top sample results in has a porosity of 0.56 and the middle sample of 0.58. ~~This leads to minor differences in plant available water (PAW, table 3), which decreases from the surface (0.26 m³ m⁻³) downwards (0.23 and 0.24 m³ m⁻³).~~ Overall, the PAW is greater soil physical properties reveal a higher PAW at the windbreak in comparison to the blackberry cropped area.



410

Figure 3. Soil water characteristic curves (vol. water content theta vs. soil suction pF) of undisturbed soil profile samples taken at different depths at the monitoring location within the windbreak rooting influence, adjacent to the soil moisture sensors. The values (dots) were taken during the drying process of the sample under laboratory conditions and parameterized with the PDI model (lines). Lines in grey represent additional undisturbed soil samples (darker shade are the upper samples, dashed line represents the WB samples).

415



420

Figure 3. Various soil characteristics of the undisturbed samples. The left panel (a) shows soil water characteristic curves (vol. water content theta vs. soil suction pF) of undisturbed soil profile samples taken at different depths at the monitoring location within the windbreak rooting influence, adjacent to the soil water content sensors. The values (dots) were taken during the drying process of the sample under laboratory conditions and parameterised with the PDI model by Peters (2014) (lines). Lines in grey represent additional undisturbed soil samples (darker shade are the upper samples, dashed line represents the WB samples). The shaded boxes illustrates the area of the PAW (plant-available water storage). The right panel (b) displays averages (bars) and ranges (lines) of different properties of the additional soil samples from March 2022: Soil hydraulic conductivity (Ksat), porosity and water content at field capacity (FC).

425

3.2.2 Topsoil transect samples

430

Both carbon and nitrogen contents ~~decrease~~decreased with increasing distance from the alder windbreaks. The highest values reaching a carbon content of 9 % C and nitrogen content 0.6 % N ~~are~~were found within the windbreaks, whereas contents of 3 % C and 0.3 % N were measured farthest from the windbreaks (fig. 4). The value range of the carbon-to-nitrogen (C:N) ratio is narrower in the vicinity of the alders compared to areas situated further from the tree line.

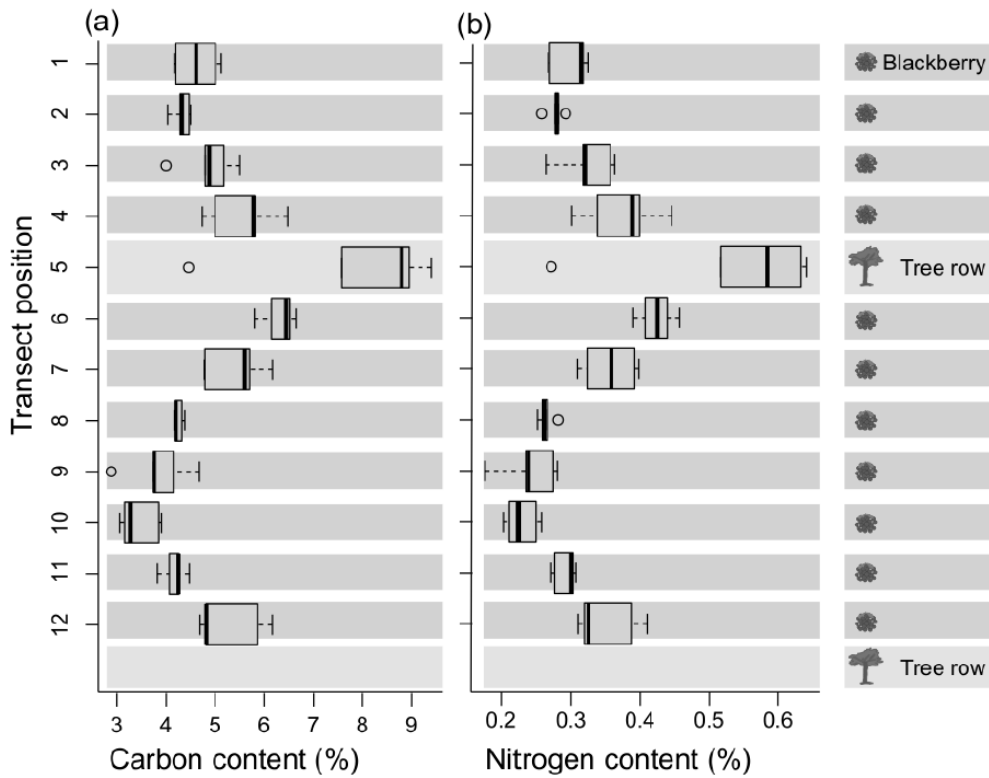


Figure 4. Carbon (a) and nitrogen (b) content of the five averaged transect topsoil (0-5 cm) samples.

435 3.3 Soil water monitoring

3.3.1 Volumetric water content and matric potential

All sensors captured the drying processes during the summer months, which ~~generally dominated~~ dominated the soil ~~moisture water content~~ and matric potential measurements (fig. 2). ~~Differences in the observations occur~~ The water content differed with depth and ~~between location and depth~~ the two measurement locations. At both locations (blackberries and windbreak), the upper soil ~~moisture sensors~~ water content was consistently ~~measured less water content~~ lower than the sensors that at greater depths. In addition, the soil ~~moisture values are~~ water content was generally ~~slightly~~ higher at the blackberry location (31.1 %) compared to the measurements at the windbreak (24.9 %). Reactions to rain events ~~are were~~ observable; however, the magnitude of the reactions ~~differs~~ differed between ~~sites~~ locations, events and sensors and is described in more detailed in section 3.3.3. ~~The Observed~~ matric potential ~~observations~~ also ~~follow~~ followed the rainfall dynamics and ~~grew substantially~~ during the drying of the soil ~~during in~~ the summer ~~and down while~~ not ~~reach~~ reaching the PWP (pF = 4.2 or -1500 kPa). ~~The Note that the~~ matric potential time series of the top sensor ~~is was~~ heavily influenced by daily fluctuations ~~relating well to incoming solar radiation~~ (fig. 2), which become more pronounced when the soil ~~reaches~~ reached drier conditions (< -500 kPa). The two deeper sensors also ~~display~~ displayed this signal, but it ~~is was~~ more attenuated.

3.3.2 Root water uptake

The ~~calculation of the~~ daily root water uptake ~~from soil moisture observations (fig. 5) calculation~~ was not successful on many days. ~~At the windbreak location, estimation of RWU (fig. 5) was not possible~~ leading to missing values for 48 % of the ~~points~~ observations (one value per sensor per day), ~~while~~ at the ~~windbreak and 56 % at the~~ blackberry location ~~for 56 %~~. Missing days were spread over the entire measurement period, with only four days of RWU estimates available from all ~~observation~~ eight sensors. At the windbreak ~~this occurrence was~~, gaps occurred most frequently ~~observed~~ in the topsoil (20-45 40 cm) whereas at the blackberry location it occurred more often for the ~~sensors located at~~ deeper ~~sensors~~ depths (40-60 cm,

60-80 cm). ~~These missing days are spread over the entire measurement period. Only four days had RWU estimates available from all eight sensors. A further number of On days occur with no/without missing values per sensor location (21 days at the windbreak, 14 days at the blackberry location). On these days, we observe that at), 44 % of the windbreak estimated RWU primarily occurred at the depth of within 20-40 cm (44 %), whereas within the blackberry crop, followed by 28 % in the top 0-20 cm of the soil profile (70 %). RWU occurrence at the windbreak is rather uniformly distributed throughout. In the blackberries 70 % was abstracted from the profile. On top 0-20 cm. Note that, on the four days with complete sensor data, the estimated RWU is always was consistently greater at the blackberry location when compared to at the windbreak location (12 Oct.: 0.56 mm d⁻¹ < 0.82 mm d⁻¹, 13 Oct.: 0.72 mm d⁻¹ < 0.85 mm d⁻¹, 18 Oct. 0.66 mm d⁻¹ < 1.22 mm d⁻¹, 21 Nov.: 0.4 mm d⁻¹ < 1.17 mm d⁻¹).~~

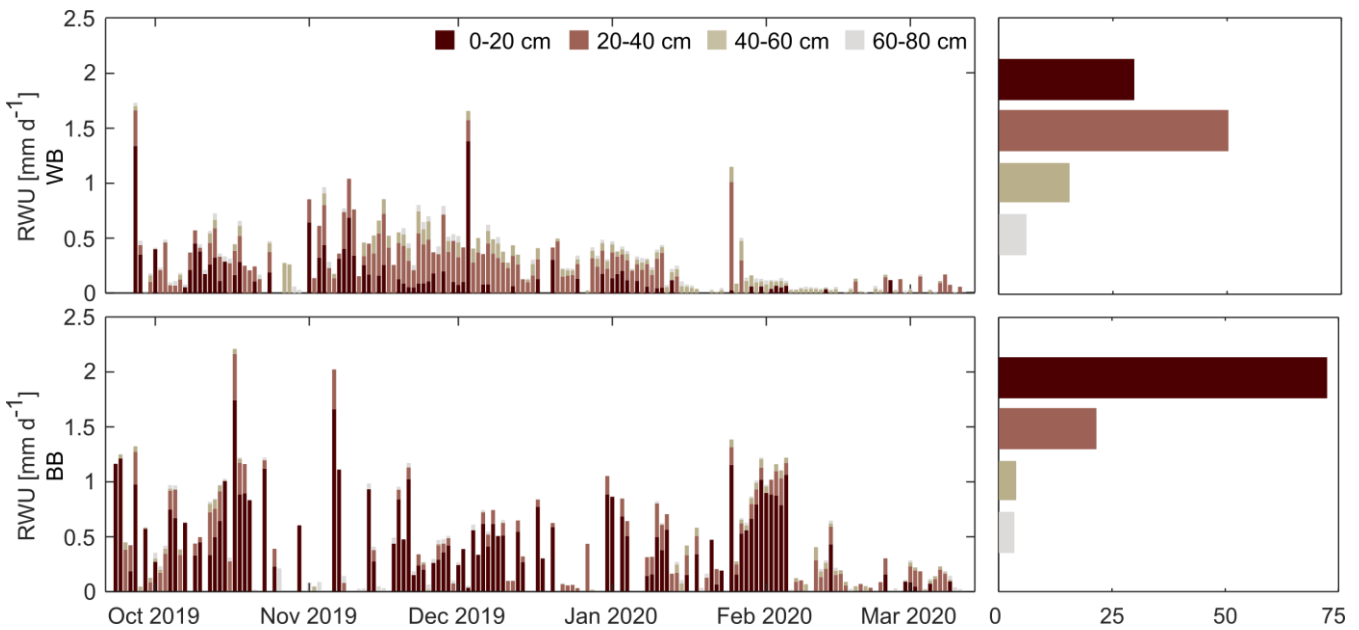


Figure 5. Stacked daily root water uptake (RWU) at the windbreak (WB) and blackberry (BB) location estimated from water content measurements at respective depth integrals. Panels on the right show how much each depth interval contributes to overall RWU [%].

~~The evaporative fraction was calculated. Neglecting water storage in the trunk, RWU provides a rough transpiration estimate and allows together with the estimated PET the calculation of the water limitation factor. Doing so for the days where RWU was available for at least all four sensors at one location (29 instances) and resulted yielded in a mean value of 0.098 (range: 0.058 – 0.223) at the windbreak and of 0.128 (0.034 – 0.230) at the berries. This indicates that transpiration is strongly water limited.~~

3.3.3 Event-based analyses

~~We defined. When defining a rain event as a minimum accumulated precipitation of 2 mm and uninterrupted/continuous rainfall periods of less than 6 hours. Applying these criteria, we identified thirteen 13 distinct events during the monitoring period (fig. 2, table 1, fig. A1). The strongest most precipitation during one event accumulated a total of 118 mm of rainfall within a 21 hour period and occurred on 25 October 2019. Two days later another storm delivered 38 mm of rainfall over 37 hours, making it the second-largest event. Two more events with precipitation exceeding 10 mm were recorded, while the smallest event captured 2.5 mm of rainfall on 8 October 2019. Across all events, soil moisture/water content reactions are rather immediate throughout the different sensors. Figure 2 presents a combination of accumulated precipitation and changes in cumulative soil moisture/water content storage for some-selected events (the largest two events in amount of rainfall, (24 and 27 October 2019, fourth and fifth event) and one smaller event (20 December 2019, tenth event). Note that shows soil moisture~~

exceeding rainfall), highlighting variations accumulated total storage increase was for all events greater in the blackberries than in the reactions windbreak. During the smaller event in soil water uptake. In the figure 2 it even increased local rainfall supply, probably due to lateral flow processes. The two largest events (> 30 mm), a signal of lead to an increasing soil moisture is observable water content until the sensors at the depth of 40-60 cm. Accumulated total storage change was during the last storm at both sites, clearly smaller than the rainfall supply, while during the fifth event (fig. 2, bottom middle panel) the increase came close to the total rainfall at the blackberries. There is a was furthermore a clear difference in the timing at which sequence how the deeper sensors detect the rise in water content responded. On 25/24 October 2019, there is was a gradual downward percolation of water, whereas as reflected in the sequential storage response. Whereas on 28/27 October 2019, all three upper sensors showed a simultaneous increase in soil moisture water content, particularly at the blackberry location. Furthermore/Moreover, during the latter event, the soil did not retain the water; instead, soil moisture water content rapidly declined once the precipitation ceased, which differed from the behaviour in response of the first event.

3.4 Windbreak characterisation

3.4.1 Windbreak properties

The windbreak consists of 40 aligned trees spaced evenly and neither tree without gaps nor mortality were present. Table 43 provides information on the tree structure and QSM-derived attributes. Great A large degree of heterogeneity of the windbreak's tree structure shows is demonstrated by DBH measurements (diameter at breast height, standard measurement at 1.3m above ground) ranging from 7.7 to 33.3 cm and tree height variations between 4.3 and 13.3 m. The QSM optimisation provided precise estimates of tree heights (CV% ca. 1 %). Tree point clouds classified with high occlusion had higher uncertainties in QSM-derived tree parameters. The estimated LAI-dependent interception storage capacity yielded to 0.664 mm on the alder leaves, if assuming a LAI value of 6.64 m² m⁻² based on a leaf spacing of 2.5 cm for trees within the windbreak row (table 43).

Excluding the edge trees exhibiting a more open grown form, the total wood volume was found to be 617.4 ± 0.6 m³ m⁻¹ ("per linear metre of windbreak"), including 352.3 ± 0.4 m³ m⁻¹ of branch wood. The estimated dry total biomass (trunk, branch, coarse roots) amounted to 259.3 kg m⁻¹. The variation of biomass stocks above and belowground is are noted in table 43.

The shadow model suggested a substantially reduced solar insolation at the soil surface due to shading effects of the trees (up to 75 % of incoming solar radiation intercepted). This shading effect spread up to 4 m towards the north (uphill) and up to 9 m towards the south (downhill). Along the east-west axis, the shading effects were greater in size but less intense than in the north-south axis. Specific zones of minimum radiation (≈ 5 MJ m⁻²) occurred within the windbreak, mainly towards the southern side.

Table 3. The calculation based on the work by Gholz et al. (1979) led to smaller values of biomass with total aboveground biomass being 95.7 kg and 99.6 kg and belowground 21.6 and 22.4 kg for the days in March of 2020 and 2021 respectively. Therefore, the incremental biomass is 4.7 kg. Dividing this by the yearly PET led to a WUE of 0.0042 g g⁻¹ if considering the total biomass and 0.0027 g kg⁻¹ if considering only the stem biomass (such as in Dye et al. (2008)). Scaling the WUE up to the average estimated biomass of 259.3 kg per metre of windbreak estimated by the QSM optimisation results in 62,378.7 L (62.38 m³) of water required to produce this amount of biomass.

Table 4. Windbreak properties derived from tree data (QSM based) and additional point cloud methods.

Group	Property	Unit	Values	Description
-------	----------	------	--------	-------------

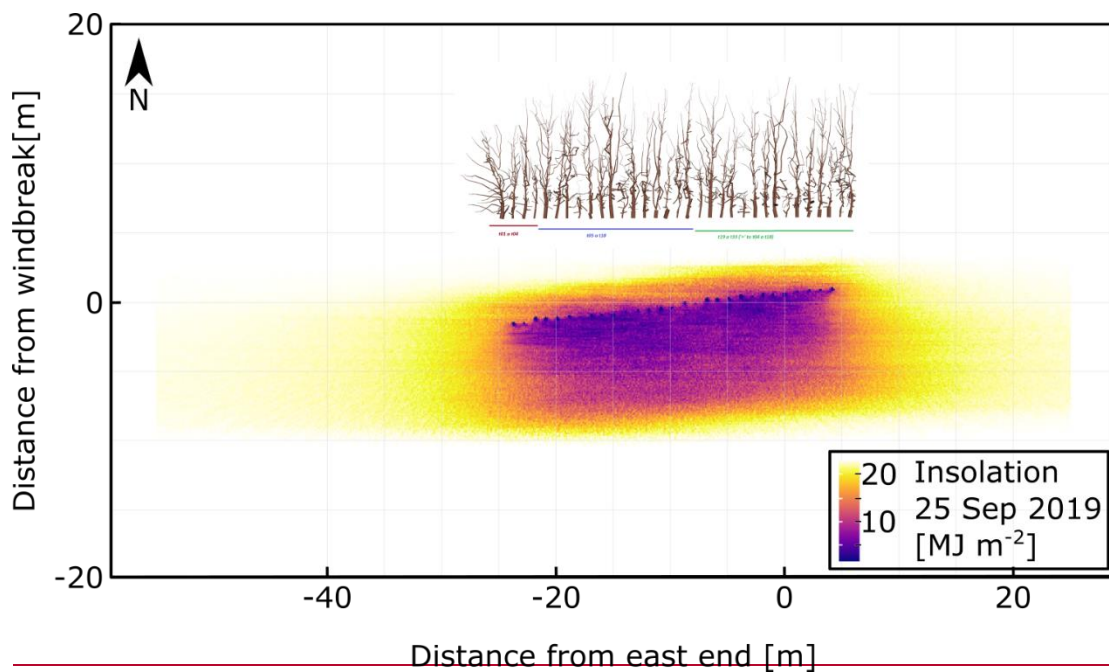
Structure	Orientation	-	ENE-WSW	Windbreak cardinal direction
Windbreak properties derived from tree data (QSM based) and additional point cloud methods.				
Group	Property	Unit	Values	Description
Structure	Orientation	-	ENE-WSW	Windbreak cardinal direction in half wind
	Tree Count	count	40	Number of trees in the windbreak
	Tree Spacing	m	1	Planting spacing (trunk-to-trunk)
	Width	m	9.46	Measured windbreak width
	Length ttt	m	39	Measured trunk-to-trunk windbreak length
	Length ctc	m	48	Measured crown-to-crown windbreak length
	Plant Coverage	-	0.819	Ratio of the min. bounding box and the alpha-hull of leaf points
Volume	Trunk	$\frac{\text{Lm}^3}{\text{l}}$ m ⁻¹	128.0.1	Trunk volume per meter linear metre of windbreak
	Branch	$\frac{\text{Lm}^3}{\text{l}}$ m ⁻¹	352.30.4	Branch volume per meter linear metre of windbreak
	Root	$\frac{\text{Lm}^3}{\text{l}}$ m ⁻¹	1370.1	Root volume per meter linear metre of windbreak
	Total	$\frac{\text{Lm}^3}{\text{l}}$ m ⁻¹	617.40.6	Total volume (trunk, branch, coarse roots) per meter linear metre of windbreak
Biomass	Aboveground	$\frac{\text{Kkg}}{\text{m}^1}$	201.7	Aboveground biomass (trunk, branch) per meter linear metre of windbreak
	Belowground	$\frac{\text{Kkg}}{\text{m}^1}$	57.6	Belowground biomass (coarse roots) per meter linear metre of windbreak
	Total	$\frac{\text{Kkg}}{\text{m}^1}$	259.3	Total biomass per meter linear metre of windbreak (without leaves)
Foliage	Leaf Mass	$\frac{\text{Kkg}}{\text{m}^1}$	3.46 ; 4.12 ; 5.12	Leaf dry mass per windbreak meter metre (leaf spacing 3, 2.5 and 2 cm)
	Leaf Area	m ² m ⁻¹	45.00 ; 53.69 ; 66.64	Leaf area per windbreak meter metre (leaf spacing 3, 2.5 and 2 cm)
	LAI	m ² m ⁻²	5.56 ; 6.64 ; 8.24	Leaf area index (with leaf spacing 3, 2.5 and 2 cm)

530

3.4.2 Shade-cast simulation with the shadow model

Figure 6 illustrates the total solar radiant energy impacting the ground throughout the day on 25 September 2019. The presence of the windbreak reduces the insolation at the soil surface due to shading effects near the trees substantially (up to 75 %, close to the windbreak). These shading effects spread up to 4 m towards the north (uphill) and up to 9 m towards the south (downhill). Along the east-west axis, the shading effects are greater in size but less intense than in the north-south axis. Specific zones of minimum radiation ($\approx 5 \text{ MJ m}^{-2}$) occur within the windbreak, mainly towards the southern side.

535



540 **Figure 6.** Insolation at ground plane modelled with the tree structures of the windbreak in leaf-off conditions for the entire day of 25 September 2019.

4 Discussion

4.1 Influence of windbreak on Windbreaks influence dominant processes of the water balance

545 In the following we discuss the various processes of the water cycle occurring at the soil-atmosphere boundary on a plot scale and how they are influenced by the windbreak. Tracking water input, we investigate water movement into and within the soil, water redistribution and its pathway out of the study area.

4.1.1 Water input: Precipitation, irrigation, interception

550 The measurement period falls into the South African summer months including January, which is historically the driest month of the year with on average 16 mm (here 9.1 mm) of precipitation. The total precipitation recorded was 245 mm and partially covers the annual average of 742 mm of the region (Meadows, 2015; Veste et al., 2020). Accurate irrigation volumes and frequencies were not available, with the assumption that irrigation volumes were consistent throughout the season, the trickle irrigation system may provide a weekly water input of up to 60 mm. The irrigation amount significantly contributes to the overall water balance, exceeding the long-term average of 132 mm of the wettest month.

4.1.1 Windbreaks alter microclimatic precipitation patterns

555 The measurement period fell into the South African summer months including January, which is historically the driest month of the year with on average 16 mm (in our study: 9.1 mm) of precipitation. Total precipitation sum was 245 mm (30-year average for the same period is 206.5 mm) and partially covered the annual average of 787 mm for the region (Meadows, 2015; Veste et al., 2020; Climate-Data.org, 2024). Accurate irrigation volumes and frequencies were not available, with the assumption that irrigation volumes were consistent throughout the season, the trickle irrigation system may have provided a weekly water input of up to 60 mm. In comparison to the precipitation, this accrued to a total of 240 mm per month, which can be considered to significantly contribute to the overall water balance, exceeding the long-term average of 132 mm of the wettest month.

560 By intercepting rainfall, and storing part of it on leaves and branches, trees reduce the amount and ~~velocity of water running on~~ kinetic energy of rainfall reaching the surface, and hence, its availability to vegetation below the crowns of the windbreak

565 trees. The capacity of trees to store precipitation depends on specific characteristics, such as crown density and leaf surface
area, additionally the size and dynamic of the rainfall event itself and the prevailing climatic conditions (Baptista et al., 2018;
Schumacher and Christiansen, 2020). We found that the tree branch volume was approximately three times higher than the log
volume, and consequently the total wood surface area was high. This indicates a strong branching of the windbreak structure,
and therefore, dense vegetation (i.e.g. low porosity). ~~The~~Our assumption considers that interception storage capacity is directly
570 proportional to LAI, making this variable valuable for analysing different forest types and tree species, even under varying
growth conditions (Schumacher and Christiansen, 2020). A LAI storage capacity of 0.664 mm per event results in a total
interception of 8.5 mm for all events during the measurement period, accounting for 3.5 % of the total precipitation for the
measurement period. ~~This value is comparable to Muthuri et al. (2004) who reported 5 % interception of *Alnus acuminata*
during a five year simulation exercise. It is important to consider that our value may underestimate the total interception as
575 events smaller than 2 mm are not considered.~~ It is important to acknowledge that our value may underestimate the total
interception, as events smaller than 2 mm are not considered. Including all events (32 events with precipitation > 0.1 mm)
would yield an interception of 21.2 mm or 8.6 % of rainfall. Interception is generally influenced by two factors, 1) vegetation
characteristics such as density, age, and height; and 2) precipitation properties such as intensity, duration and frequency. The
literature gives interception values of, for example, 22 % of yearly rainfall for temperate deciduous broadleaf forests, which
580 would lead in our case to 53.9 mm for the measurement period or 173 mm for a whole year (Dingman, 2015). Interception in
windbreaks is likely to be lower than in closed-canopy forests as branches are all the way down the canopy exposed to wind
movement, thereby shedding additional water from the canopy. Lower branches in closed canopies are likely to experience
less movement and can therefore hold water on canopy surfaces until it is evaporated.

The LAI values were higher than those typically found in shrublands (approximately 2.0) and similar to those found in
585 temperate and tropical forests as well as tree plantations (Bréda, 2008). Overall, we observed a higher proportion of
~~precipitation water retained~~rainwater stored in the soil at the blackberry location in contrast to the windbreak location, where
on average 63 % and 54 % of ~~rain~~the rainfall reached the soil column, respectively. This can ~~be~~ potentially be attributed to
interception differences between the two locations. The difference between the two locations is 26.5 mm for the entire period,
which ~~closely~~ aligns with the interception amount of 40 mm per year reported~~stipulated~~ in the literature for alder species
590 (Muthuri et al., 2004). However, the alternated wind field due to the obstacle in the flow path, might also cause a change in
the precipitation pattern at and around the windbreak. Häckel (1999) state an increase of up to 15 % in precipitation behind
the obstacle (until up to 10-times plant height) and a reduction of 10 % directly at the windbreak.

4.1.2 Water movement: Infiltration, Windbreaks carry potential to buffer surface runoff and subsurface flow whereby reducing erosion

595 Water movement processes ~~on, into and within the soil,~~ such as infiltration, surface runoff and lateral subsurface flow, can be
observed during and after precipitation events, but soil physical properties can equally indicate hydrological behaviour.
Infiltration determines the splitting of rainfall into surface runoff and soil water fractions. ~~The measured~~Observed Ksat values
(302.3 mm h⁻¹ ± 191.3 mm h⁻¹) varied in the range of silty soils. Great heterogeneity of topsoil Ksat (263.1 mm h⁻¹) from is
600 expected due to the difference between the soil in the berry rows (lightly packed soil profile samples is greater than the observed
, flattened) and in-between the rows (compacted, rock fragments, steeper parts) and was confirmed by a nearly threefold
average at the blackberry location compared to the windbreak. Ksat values exceeded maximum precipitation intensities (max.
82.6 mm h⁻¹). High Ksat values from the undisturbed transect samples indicate favourable) at both locations, providing
favorable conditions for water infiltration while Ksat exceeding precipitation intensities suggests into the soil. The porous soil
inhibited a particularly high air capacity compared to common fine-pored soils. Both indicate that the soil can absorb all the
605 precipitation. However 21 % of infiltrated water was not held against gravity, i.e. not stored in the topsoil, and therefore, drained

a substantial part into deeper soil layers. The water percolated quickly downward in the topsoil (about 16 cm h⁻¹ for Ksat near the windbreak and 44 cm h⁻¹ for the blackberry crop).

Nevertheless, we did observe instances (event number 1, 5, 9, 10, 11; see also table 1) where soil water storage changes exceeded the precipitation input. ~~The event plot as illustrated in figure 2 illustrates instances where soil storage change exceeded precipitation intensity, indicating the formation of.~~ This can be attributed to either surface runoff ~~due to or lateral soil water redistribution.~~ In the first case, the soil reached saturation or infiltration excess. ~~As a result, the absolute amount of water reaching the soil is lower, directly impacting the availability of water in the root zone (Schumacher and Christiansen, 2020), which we observed in the analysis of the precipitation events. In addition, the~~ and therefore, water did not percolate into the soil, leading to its accumulation and downslope movement on the soil surface. The matric potential surpassed the FC threshold during the late October and December events, ~~both (event numbers 4, 5 and 17-12),~~ confirming the occurrence of surface runoff. ~~Either the water moved on the surface until it was lost to the study site or it infiltrated at a different location into the cropped area. Due to the aforementioned heterogeneous surface between the rows, it is likely that surface water formed on the compacted and steeper parts of the slope and infiltrated in the flattened area around the blackberry plants or was buffered by the windbreak. In general, for most events, the cumulative soil water storage at both locations did not align with the recorded precipitation amount, supporting the occurrence of lateral redistribution at the soil surface or subsurface. In the case of lateral subsurface flow, i.e. soil water redistribution, water moved horizontally instead of percolating downwards when reaching a less permeable soil layer. This was evidenced by a substantially decreasing Ksat with depth (at 0.5 m Ksat = 3.2 mm h⁻¹) and might benefit the windbreak.~~

The often-observed delayed responses of soil water content changes after the onset of a precipitation event can be an indicator for both infiltration after surface runoff and lateral redistribution. Additionally, the simultaneous reaction of the deeper sensors with the shallower ones is evidence for preferential flow through e.g. macropore input (fifth event in table 1, bottom middle panel in fig 2).

The distribution of nitrogen and carbon concentrations (fig. 4) ~~supports this~~ supported the occurrence of lateral redistribution, as the enrichment around the windbreak ~~is was~~ likely a result of a combination of erosion from downslope surface runoff and the accumulation from the trees themselves (see section 4.2.2). ~~Similarly, We observed very high precipitation intensities (max. observed 82.6 mm h⁻¹), which probably produced surface runoff with high kinetic energy, and therefore, had the potential to produce splash or sheet erosion even in cohesive soils. Possibly, the windbreak may not be apparent in the soil water content changes but~~ downslope erosion of fine soil could ~~also~~ explain the unexpected observed lower Ksat values near the windbreak ~~in the samples from 2022~~, which is underpinned by larger bulk density and lower porosity at the windbreak. ~~However, we could not specifically find texture differences in the undisturbed soil samples from 2022 between the two locations that would confirm this hypothesis. We did not find considerable texture differences between the two locations, but fine particles could be masked through the formation of aggregates (Jackisch et al., 2017). Carbon addition may also increase and stabilise aggregates in fine-grained soils.~~

~~Infiltration occurs at similar rates and the flow is likely dominated by macropores, as evidenced by the immediate and minimally delayed response of the sensor at lower depths upon the onset of water input (event number 5 in table 1, bottom middle panel in fig 2). As interception reduces the amount of water entering the soil, the amplitudes of changes in soil water storage are less pronounced at the deepest windbreak sensor. In general, for most events, the cumulative water storage in the soil at both locations does not align with the recorded precipitation amount, supporting the occurrence of lateral redistribution at the soil surface or subsurface.~~

4.1.3 ~~Water output: Actual~~ Windbreaks reduce crop evapotranspiration estimation

Root water uptake calculations did not work for approximately 50 % of the data points due to the absence of an ~~increased~~ decrease in the soil ~~moisture~~ water content time series during the ~~night~~ day, which results in a typical step-shape curve

that is the necessary for RWU estimation (Jackisch et al., 2020). The influence of the irrigation on these estimations is ~~also~~ unclear, although it should be consistent at both locations. ~~For these reasons, thus, allowing relative interlocal comparison.~~

650 ~~Nevertheless,~~ we ~~consider~~ are cautious about the achieved RWU estimates at this site ~~with great care~~ due to missing data.

The RWU pattern differed between the two locations (fig. 5) with a higher proportion occurring in the topsoil at the blackberry location and a more evenly distributed uptake around the 20-40 cm depth within the windbreak. This indicates that the alder trees draw water from a broader range of soil horizons than the blackberry crop. The perennial blackberry plants have a main root, which can extend vertically to a maximum depth of 1.5 m (depending on soil type) and have numerous secondary roots, growing horizontally for 30-60 cm before descending vertically (Bruzese, 1998). Alder trees are water-demanding species with high evapotranspiration rates due to the absence of mechanism to control stomatal regulation (Herbst et al., 1999). It is unclear whether the studied *A. cordata* exhibits deep rooting on the thin and rocky soils of the steep slope at our study site (80 cm soil depth at our exemplary soil profile). However, it is reasonable to assume that the species can reach the deeper soil layers due to its rooting potential. ~~Kutschera and Lichtenegger (2002) reported that *Alnus glutinosa* (L.) Gaertn. from the same family as the *Alnus cordata* is a deep-rooting plant in waterlogged soils, with its roots reaching a depth of about 120–150 cm (Kreutzer, 1986).~~

660 ~~If the trees tap water sources below 80 cm, it would not have been captured with the installed measurement devices which in turn would explain why we observed much less water uptake at the windbreak when compared to the blackberries. Without additional information, it is difficult to determine whether the observed differences in RWU patterns are due to different rooting depths between the two species. In addition, the~~ The RWU cannot be used to estimate evapotranspiration of the windbreak. However, the ~~evaporative fraction~~ water limitation factor was estimated for days with complete sensor data and gives an idea of how much of the available radiation energy is used for RWU, and therefore, transpiration and plant growth. For the days under consideration less RWU (~~evaporative fraction~~ f_w : 9.8 %) occurred at the windbreak in contrast to the blackberry location (~~evaporative fraction~~ f_w : 12.6 %), which could be caused by a) a lack of RWU estimates due to unsuitable soil ~~water limitation (content time series, or simply~~ b) the installed sensors not being installed in

665 ~~an incorrect~~ suitable location (adjacent to root or deep enough) and therefore not sufficiently capturing the RWU). Interestingly, the Budyko aridity index ~~indicates~~ indicated a shift from a water-limited to an energy-limited system when considering the additional irrigation input (changing from 3.7 without irrigation to 0.65 with irrigation). This is confirmed by the matric potential sensors, which ~~show~~ showed that the plant ~~does~~ did not reach the PWP (fig. 2), i.e. the point at which water fluxes are nearly immobile. Water becomes a limiting resource. ~~for many plants already at lower absolute matric potential values.~~

670 The water supplied to the system by irrigation is was the dominant component of the water budget and as a consequence, the AET is was closer to the PET. Consequently, estimations of wind and sun shading effects can provide an idea of the AET at the field site. ~~In fig. 6, a~~ simulation demonstrates demonstrated the windbreak's potential reduction of solar radiation on the ground, which can be up to 75 % in the immediate vicinity of the windbreak on a sunny day, as observed on 25 September 2019. The PET is was estimated at 23.310.8 mm for the entire day from the meteorological data without shading, however,

680 some areas of the blackberry crop did experience the shading effect of the windbreak. For instance, on the southern side of the windbreak, on a part of the field where the solar energy is reduced by 50 % for approximately 6 ~~hours~~ h, the daily PET ~~decreases~~ decreased from 23.310.8 to 14.86.9 mm d⁻¹. On the northern side of the windbreak, where the blackberries and soil ~~are~~ were protected from the southerly winds occurring that day (depending on the distance up to a 30 % reduction in PET) assuming a 15 % reduction in PET due to wind speed reduction the PET ~~reduces~~ reduced from 23.310.8 to 49.89.2 mm d⁻¹. If

685 both effects were to occur on the same side, the cumulative impact could lead to a reduction to 12.65.8 mm d⁻¹, resulting in an AET that is 54 % of the PET.

While this example calculation is based solely on theoretical values and lacks actual data for ~~comparison~~ validation, it underscores the importance of the windbreak in a water-scarce region. A 30 % reduction in water demand can be crucial for the sustainability of natural and agricultural ecosystems. In a nearby vineyard, Veste et al. (2020) measured a 20 % reduction in wind speed and ~~ET~~ evapotranspiration due to tree shelterbelts. For the sake of completeness, it should be noted that sunlight

690

is essential for the growth of the blackberry crop, and excessive shading may adversely affect growth, and thus, the yield of the field, hence, a detailed assessment of shading effects is crucial ~~for an integral assessment. It is likely that the reduction in insolation around the windbreak is shifted towards the south (downhill in the case of the given study site), as the simulation only allows shade projections on a flat terrain. Therefore, we would expect the insolation reduction to expand down the slope and decrease as one moves up the hill.~~ Shading is predominately a factor of height, volume and porosity of windbreak crowns, other structures in the landscape, aspect and slope.

4.2 Windbreak-induced Windbreaks induce benefits for water availability and nutrient cycles ~~in the landscapedistribution~~

4.2.1 Overall Windbreaks potentially improve soil water storage capacities

One way to estimate plant-available water is through the inspection of the water retention curve and different storage capacities quantified by soil hydraulic properties (fig. 3). As previously mentioned, we observed high porosity and high air capacity (21 %) in the soil, determining that a large fraction of the shallow soil drained instead of storing the water. It was also quite striking that K_{sat} is substantially larger in the blackberry soil, even though if estimated based on texture and porosity, it would appear to be similar. This clearly indicates that structural effects in the soil with a high fraction of fine pores holding water, but also a fraction of well drainable pores, are allowing water to percolate.

~~In contrast to our samples which displayed higher topsoil organic matter concentration but with similar PWP, Interestingly, the three different volumetric pore compartments of the soil 1) air capacity or drainable volume, 2) effective field capacity PAW and 3) wilting moisture PWP are nearly the same (approx. 20 %). This could be beneficial to the ecosystem: By percolating further into the soil, water is protected from evaporation. A less permeable layer deeper in the soil profile can collect the percolated water, plants that are able to root down to such a depth can benefit from this source: The fraction that is beyond the wilting point inhibits the same size as the fraction that percolates down and is available for plants at greater depths. Usually, the drainable fraction is much smaller in fine pore soils.~~

Bogie et al. (2018) found significant differences in water retention at the PWP ~~due to the potential of carbon addition to increase and stabilise aggregates in fine grained soils~~ alongside changes in surface properties brought about by higher CEC of organic matter in coarse soils. ~~The PWP This is also similar between windbreak and blackberry locations (both approximately 17 %) according to the similar in contrast to our samples, which had higher topsoil organic matter concentrations in the undisturbed samples. concentration, but similar PWP.~~ The retention curves ~~differ~~ differed mainly in the wet range and ~~are were~~ rather similar in the dry range. The spread in the wet range ~~is was~~ greater for the lower samples, while the upper samples ~~are grouped a bit closer together and have varied less and had~~ slightly steeper curve shapes. ~~The soil profile samples show a clear decrease in plant available water with depth, resulting primarily from the decrease in FC water content (table 3).~~ In the ~~additional samples from 2022 the topsoil plant available water is larger~~ topsoil PAW was greater at the windbreak (19.7 %) than in the blackberry crop (16.4 %), generally resulting in a higher potential to retain water in the soil near the windbreak. The deeper samples ~~show displayed~~ very similar values for PAW (19.3 and 19.2 %). As shown in the previous section, overall, less water ~~is reachingreached~~ the soil at the windbreak even though the potential to store it based on texture is greater.

Both the volumetric water content (at both locations) and matric potential (measurements at the windbreak only) observations consistently show that the topsoil is drier than the soil at greater depths (fig. 2). The drier surface is due to evaporation of soil water combined with water withdrawal by plants from the topsoil, whereas the deep layers are not affected by evaporation and only to some extent by root water uptake. The former can be seen in the observations of the matric potential, which exhibited pronounced daily fluctuations ~~at the surface that correlate well with the solar radiation.~~

The matric potential sensors did not reach the PWP of -1500 kPa during the measurement period. The uppermost sensor reached values below -1000 kPa for 53 of the 4200 data points, all occurred between January and March mostly around midday (range from 11:00 to 17:00, with an average at noon). This coincides with the times of the day when the field site is irrigated

(informally for a few hours every two to three days during the summer). Both the time series of matric potential and supplemental irrigation ~~indicate~~indicated that sufficient water was available throughout the period and the plants did not experience any severe water stress.

The soil ~~moisture~~water content time series recorded at any location frequently reached the PWP (estimated from retention curves: the top sensor at windbreak location for 86 % and top sensor at the blackberry location for 20 % of 4200 hourly data points respectively). The main difference between the locations is that at the blackberry location the PWP ~~is~~was reached only towards the end of summer (after 8 February), whereas, at the windbreak this limit ~~is being~~was reached several times throughout the observation period. We ~~are~~were more likely to trust the absolute values of the matric potential in this context, among other reasons because the volumetric water content sensors were used with the calibration provided by the manufacturer and not a field site specific ~~one~~setting, and therefore, susceptible to offset errors.

~~The trees need water for biomass growth. A rough estimation based on DBH and water use efficiency (assuming all potential energy leads to transpiration) indicates that the trees used on average around 62 m³ of water for growing to their present size. That is on average (assuming a mean estimated age of all windbreak trees to be 17 years) 3669 L m⁻² per year, clearly exceeding the yearly precipitation of 742 mm and also the water input if considering the irrigation (irrigation and precipitation: 1402 mm only for the period September to March; 1902 mm if adding irrigation to yearly precipitation). Several factors affect this approximation: 1) the trees will not maintain the same water consumption throughout their lifetime; 2) not all potential energy will result in transpiration, and therefore, water consumption of the trees.~~

~~4.2.2 Nutrient distribution and~~4.2.2 Nutrients accumulate around windbreak and windbreaks enhance carbon sequestration potential

Possible reasons for the considerably higher nitrogen and carbon concentrations in the ~~alder~~windbreak row are (a) the relocation or erosion of soil material following surface runoff in the upper and steeper parts of the slope to the flatter slope at the windbreak and (b) the continuous addition of N-rich alder biomass in form of litter fall, root exudation, and root biomass leading to higher microbial activity. Italian alder is a N-fixing tree and is able to capture atmospheric nitrogen in symbiotic root nodules (Claessens et al., 2010). There are a number of N-fixing species that seem to retard the decomposition of native soil ~~C~~carbon. Thus, this fact combined with their own root carbon productions causes the increase in soil ~~C~~carbon normally observed among N-fixing species. The bulk of the increase in soil organic carbon could ~~come~~result from dead roots arising from the ~~alder~~trees. So, erosion is probably less important than root turnover when it comes to carbon input.

An additional potential not discussed in much detail in this study is the ~~potential for~~ carbon sequestration of the windbreaks in the landscape. From the terrestrial laser scans we estimated total dry biomass ~~to~~of 259 kg ~~per metre~~m⁻¹ of windbreak. Under the rough assumption that water/woody biomass is a 50/50 split and carbon constitutes 50 % of dry biomass (Thomas and Martin, 2012); and according to the molecular weight of CO₂ we can suggest that 238 kg CO₂ equivalent (Guest et al., 2013) is sequestered in the biomass of the study alder trees. Sheppard et al. (2024) for example, showed that a poplar windbreak in South Africa of similar dimensions could store nearly 200 tons of CO₂ equivalent per km of windbreak in the aboveground portion alone. In comparison with forested land this may not be much, but as an additional carbon sink on farmland it presents a large additional potential for short to mid-term carbon storage.

5 Conclusions

Windbreaks ~~exert major and varied effects on~~play a significant role in shaping the ~~surrounding crop ecosystem in AFS. Their successful implementation and proper functioning can yield multiple benefits and heavily relies on the complex~~ water dynamics, ~~especially of their surroundings, yielding various benefits when implemented and managed effectively, particularly in water regions with limited~~ regions. ~~We observed influences~~water resources. Our investigation into their impact on the water balance utilised a range of methodologies, including analyses of sensor data and soil sampling.

775 The windbreaks not only altered local precipitation levels but also influenced its distribution. Proximal to the windbreak, precipitation input was reduced by approximately 3.5 % due to interception, while in their leeward effects can lead to up to a 15 % increase in precipitation levels due to disruptions in the wind field. These effects could explain the observed higher proportion of water being retained in crop compared to windbreak soils. However, a more precise understanding of interception storage and the water usage of trees, through multiple methods utilising and analysing sensor data and soil samples e.g. sap flow measurements or improved root water uptake estimates, is needed to refine the water balance assessment. Discrepancies

780 in soil water content may also stem from variations in hydraulic conductivity, which determine infiltration rates. Observations indicated lower hydraulic conductivity at the study windbreak compared to the blackberry location, possibly due to soil erosion during high-intensity precipitation events. Nonetheless, topsoil conditions generally favored infiltration, with a significant portion of water draining the topsoil and reaching deeper layers. Since the water at greater depths was protected from evaporation, plants might benefit by tapping water from this source. By reducing wind speeds, windbreaks reduced crop

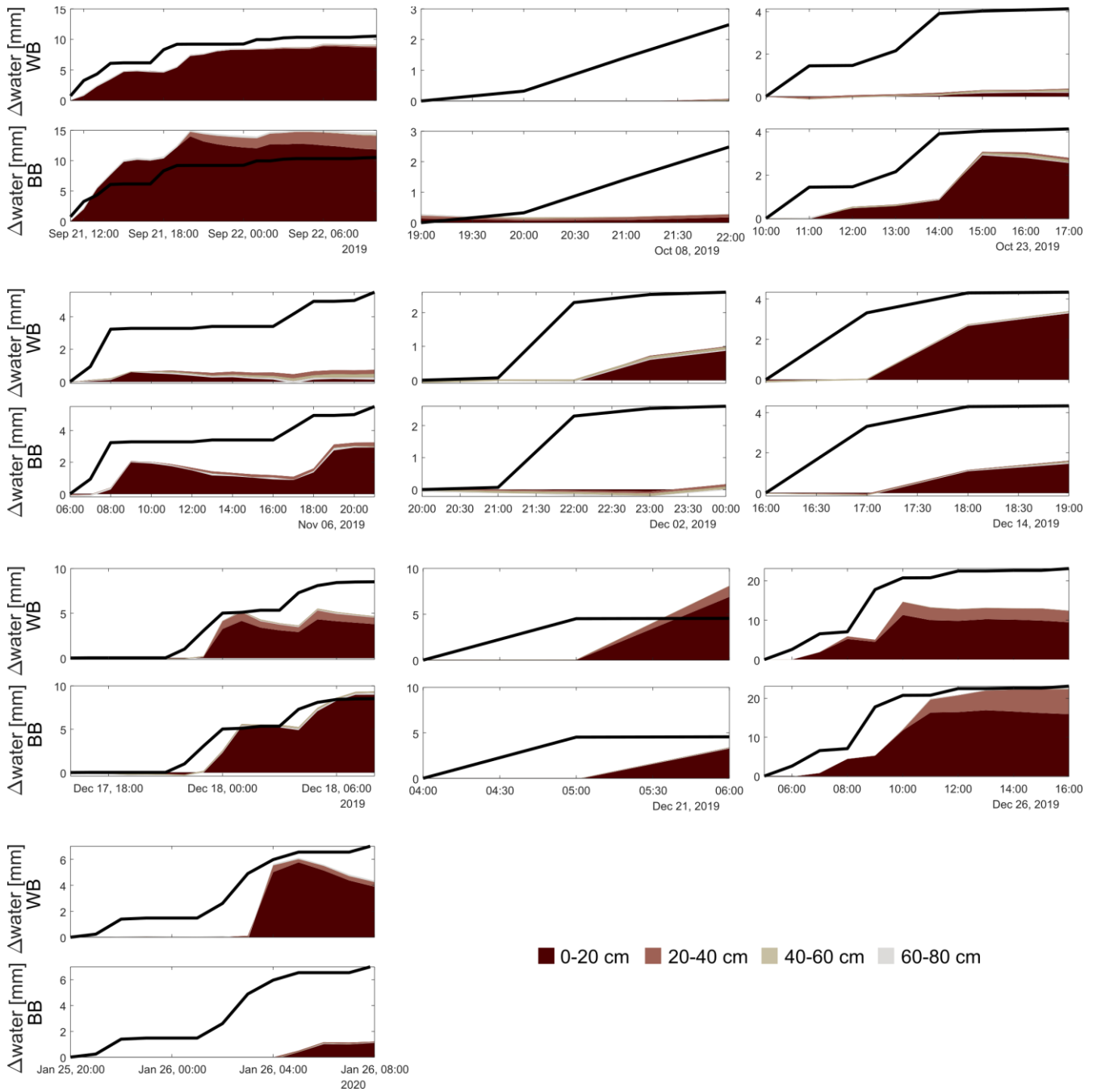
785 evapotranspiration, while irrigation shifted the system from water-limited to energy-limited conditions, leading to increased actual transpiration. This is corroborated by soil water measurements indicating no water stress in plants. Furthermore, windbreaks contributed to soil health by accumulating nutrients and enhance carbon sequestration potential in contrast to monoculture farmland i.e. traditional crop framing without trees.

790 ~~The irrigation exerted a major influence on the water balance by transitioning the entire system from water limited to energy limited, ensuring sufficient water for plant growth. The windbreak themselves reduced the water demand needed for this transition by reducing soil evaporation substantially while additionally influencing processes such as interception and water redistribution. Nutrient distribution and soil physical properties differed near the windbreak in comparison to the blackberry crop and point towards nutrient accumulation by the windbreak and the occurrence of water erosion. The carbon sequestration potential of this AFS is large in comparison to monoculture farming.~~

795 ~~Collaborative research endeavours can provide a comprehensive assessment of AFS's advantages and disadvantages. Combining methods from various disciplines draws a clearer picture of these complex systems.~~ This interdisciplinary work explored numerous aspects of AFS and acquired different perspectives, confirming hypotheses through cross-method analyses (e.g. surface runoff detection in event-based sensor data combined with nutrient distribution analysis). The combination of additional monitoring data and repetition of campaign-based measurements with modelling studies would help with closing

800 the water balance and might be able to fill remaining gaps and shed light on open questions regarding water fluxes in AFS.

Appendix A



805

Figure A1. Panels show cumulative precipitation (line) and cumulative soil water storage change of each sensor for all precipitation events not shown in figure 2, for both the windbreak (upper row) and the blackberry (lower row) location. The different colours represent the different depths of the sensors.

810

815

Table A2. Laboratory analysis of three soil samples taken adjacently to the soil water content monitoring point near the windbreak at different depths. Abbreviations are: WB P = profile, WB = windbreak, BB = blackberries, E = east, M = middle, W = west, FC = field capacity, PWP = permanent wilting point, PAW = Plant-available water. The values of the three columns from the right are estimated using the PDI water retention model (Peters, 2014). The last four rows are averages of the windbreak and berry location at the two depths.

<u>Location</u>	<u>Sample</u>	<u>Hydraulic</u>	<u>Organic</u>	<u>Bulk density</u>	<u>Porosity</u>	<u>Wat. Cont.</u>	<u>Wat. Cont.</u>	<u>PAW</u>
	<u>Depth</u>	<u>conductivity (Ksat)</u>	<u>matter</u>			<u>FC</u>	<u>PWP</u>	
	<u>[m]</u>	<u>[mm h⁻¹]</u>	<u>[%]</u>	<u>[g cm⁻³]</u>		<u>[m³ m⁻³]</u>	<u>[m³ m⁻³]</u>	<u>[m³ m⁻³]</u>
<u>WB P</u>	<u>0.0</u>	<u>263.1</u>	<u>15.1</u>	<u>1.17</u>	<u>0.56</u>	<u>0.426</u>	<u>0.178</u>	<u>0.248</u>
<u>WB P</u>	<u>0.3</u>	<u>108.7</u>	<u>9.3</u>	<u>1.11</u>	<u>0.58</u>	<u>0.367</u>	<u>0.136</u>	<u>0.231</u>
<u>WB P</u>	<u>0.5</u>	<u>3.2</u>	<u>7.3</u>	<u>1.49</u>	<u>0.44</u>	<u>0.393</u>	<u>0.169</u>	<u>0.224</u>
<u>WB E</u>	<u>0.05</u>	<u>203.3</u>	<u>6.6</u>	<u>1.19</u>	<u>0.55</u>	<u>0.368</u>	<u>0.165</u>	<u>0.203</u>
<u>WB E</u>	<u>0.28</u>	<u>94.05</u>	<u>10.2</u>	<u>1.16</u>	<u>0.56</u>	<u>0.396</u>	<u>0.168</u>	<u>0.228</u>
<u>WB M</u>	<u>0.05</u>	<u>114.5</u>	<u>13.9</u>	<u>1.19</u>	<u>0.55</u>	<u>0.364</u>	<u>0.174</u>	<u>0.191</u>
<u>WB M</u>	<u>0.26</u>	<u>111.4</u>	<u>10.3</u>	<u>1.18</u>	<u>0.55</u>	<u>0.335</u>	<u>0.164</u>	<u>0.172</u>
<u>WB W</u>	<u>0.05</u>	<u>171.9</u>	<u>14.2</u>	<u>1.19</u>	<u>0.55</u>	<u>0.373</u>	<u>0.175</u>	<u>0.199</u>
<u>WB W</u>	<u>0.23</u>	<u>426.6</u>	<u>11.5</u>	<u>1.12</u>	<u>0.58</u>	<u>0.358</u>	<u>0.179</u>	<u>0.179</u>
<u>BB E</u>	<u>0.10</u>	<u>688.8</u>	<u>11.9</u>	<u>1.01</u>	<u>0.62</u>	<u>0.322</u>	<u>0.158</u>	<u>0.164</u>
<u>BB E</u>	<u>0.25</u>	<u>186.8</u>	<u>11.5</u>	<u>1.25</u>	<u>0.53</u>	<u>0.379</u>	<u>0.180</u>	<u>0.199</u>
<u>BB M</u>	<u>0.10</u>	<u>255.7</u>	<u>12.7</u>	<u>1.06</u>	<u>0.6</u>	<u>0.327</u>	<u>0.169</u>	<u>0.158</u>
<u>BB M</u>	<u>0.25</u>	<u>189.3</u>	<u>6.9</u>	<u>1.21</u>	<u>0.54</u>	<u>0.393</u>	<u>0.176</u>	<u>0.216</u>
<u>BB W</u>	<u>0.10</u>	<u>379.8</u>	<u>9.7</u>	<u>1.13</u>	<u>0.57</u>	<u>0.346</u>	<u>0.178</u>	<u>0.168</u>
<u>BB W</u>	<u>0.25</u>	<u>413.1</u>	<u>12.0</u>	<u>1.04</u>	<u>0.61</u>	<u>0.331</u>	<u>0.170</u>	<u>0.161</u>
<u>WB</u>	<u>0.05</u>	<u>163.2</u>	<u>11.6</u>	<u>1.19</u>	<u>0.55</u>	<u>0.369</u>	<u>0.171</u>	<u>0.197</u>
<u>WB</u>	<u>0.25</u>	<u>210.7</u>	<u>10.7</u>	<u>1.15</u>	<u>0.56</u>	<u>0.363</u>	<u>0.170</u>	<u>0.193</u>
<u>BB</u>	<u>0.05</u>	<u>441.4</u>	<u>11.4</u>	<u>1.07</u>	<u>0.60</u>	<u>0.332</u>	<u>0.168</u>	<u>0.164</u>
<u>BB</u>	<u>0.25</u>	<u>263.1</u>	<u>10.1</u>	<u>1.16</u>	<u>0.56</u>	<u>0.368</u>	<u>0.175</u>	<u>0.192</u>

820 Data availability

A data publication is being submitted concurrently to this submission to ESSD journal.

Author Contribution

SH, RBR, BdT, SKH, FK, RM, JPS designed their respective field methods, conducted the field work and analysed the acquired data. SH and SKH collected and curated the data of all authors. SH and EZ prepared the manuscript with contributions from all co-authors.

825

Competing interests

One author is member of the editorial board of the journal Hydrology and Earth System Sciences.

Acknowledgements

The collection of this dataset would not have been possible without the support of Raymond O’Grady and staff at Hillcrest Berries (Pty) Ltd who permitted access and accommodated the installation of equipment and long-term measurement within a working and productive farm environment. We are very appreciative of the support. We also want to acknowledge the contribution of our colleagues at the Department of Forest and Wood Science, Stellenbosch University. Namely Anton Kunneke, Deon Malherbe and Cláudio Cuaranhua who provided invaluable knowledge of the local site conditions, logistics support, and equipment maintenance as well as data download and transfer. The research was funded by the German Federal Ministry of Education and Research (BMBF) with the grant number 01LL1803. [Some of the graphs were created using the Scientific colour map by Crameri \(2018\).](#)

References

- Albrecht, A. and Kandji, S. T.: Carbon sequestration in tropical agroforestry systems, *Agric. Ecosyst. Environ.*, 99, 15–27, [https://doi.org/10.1016/S0167-8809\(03\)00138-5](https://doi.org/10.1016/S0167-8809(03)00138-5), 2003.
- Allen, R. G., Pereira, L. S., Raes, D., and Smith, M.: *Crop Evapotranspiration – Guidelines for Computing Crop Water Requirements*. FAO Irrigation and drainage paper 56, Food and Agriculture Organization of the United Nations, Rome, Italy, 1998.
- [Climate-Data.org: https://en.climate-data.org/africa/south-africa/western-cape/stellenbosch-6770/](https://en.climate-data.org/africa/south-africa/western-cape/stellenbosch-6770/), last access: 22 January 2024.
- Baptista, M. D., Livesley, S. J., Parmehr, E. G., Neave, M., and Amati, M.: Variation in leaf area density drives the rainfall storage capacity of individual urban tree species, *Hydrol. Process.*, 32, 3729–3740, <https://doi.org/10.1002/hyp.13255>, 2018.
- Bogie, N. A., Bayala, R., Diedhiou, I., Dick, R. P., and Ghezzehei, T. A.: Alteration of soil physical properties and processes after ten years of intercropping with native shrubs in the Sahel, *Soil Tillage Res.*, 182, 153–163, <https://doi.org/10.1016/j.still.2018.05.010>, 2018.
- Bohn Reckziegel, R., Larysch, E., Sheppard, J. P., Kahle, H.-P., and Morhart, C.: Modelling and Comparing Shading Effects of 3D Tree Structures with Virtual Leaves, *Remote Sens.*, 13, 532, <https://doi.org/10.3390/rs13030532>, 2021.
- Bohn Reckziegel, R., Sheppard, J. P., Kahle, H.-P., Larysch, E., Spiecker, H., Seifert, T., and Morhart, C.: Virtual pruning of 3D trees as a tool for managing shading effects in agroforestry systems, *Agrofor. Syst.*, 96, 89–104, <https://doi.org/10.1007/s10457-021-00697-5>, 2022.
- Bréda, N. J. J.: Leaf Area Index, edited by: Jorgensen, S. E. and Fath, B. D., *Gen. Ecol. Encycl. Ecol.*, 3, 2148–2154, 2008.
- Bruzzese, E.: The biology of blackberry in south-eastern Australia, *Plant Prot. Q.*, 13, 160–162, 1998.
- Budyko, M. : *Climate and life*, Academic Press, Orlando, FL, 508 pp., 1974.
- Calders, K., Newnham, G., Burt, A., Murphy, S., Raunonen, P., Herold, M., Culvenor, D., Avitabile, V., Disney, M., Armston, J., and Kaasalainen, M.: Nondestructive estimates of above-ground biomass using terrestrial laser scanning, *Methods Ecol. Evol.*, 6, 198–208, <https://doi.org/10.1111/2041-210X.12301>, 2015.
- Campi, P., Palumbo, A. D., and Mastorilli, M.: Effects of tree windbreak on microclimate and wheat productivity in a Mediterranean environment, *Eur. J. Agron.*, 30, 220–227, <https://doi.org/10.1016/j.eja.2008.10.004>, 2009.
- Claessens, H., Oosterbaan, A., Savill, P., and Rondeux, J.: A review of the characteristics of black alder (*Alnus glutinosa* (L.) Gaertn.) and their implications for silvicultural practices, *Forestry*, 83, 163–175, <https://doi.org/10.1093/forestry/cpp038>, 2010.
- [Crameri, F.: Scientific colour maps, Zenodo, https://doi.org/10.5281/zenodo.1243862, 2018.](https://doi.org/10.5281/zenodo.1243862)
- [Dingman, S. L.: Physical Hydrology, Third., Waveland Pr Inc, Long Grove, Illinois, 643 pp., 2015.](#)
- Douville, H., Raghavan, K., Renwick, J., Allan, R. P., Arias, P. A., Barlow, M., Cerezo-Mota, R., Cherchi, A., Gan, T. Y.,

- Gergis, J., Jiang, D., Khan, A., Pokam Mba, W., Rosenfeld, D., Tierney, J., and Zolina, O.: Water Cycle Changes, in: Climate Change 2021 – The Physical Science Basis. Contribution of Working Group I to the Sixth Assessment Report of the Intergovernmental Panel on Climate Change, edited by: Masson-Delmotte, V., Zhai, P., Pirani, A., Connors, S. L., Péan, C., Berger, S., Caud, N., Chen, Y., Goldfarb, L., Gomis, M. I., Huang, M., Leitzell, K., Lonnoy, E., Matthews, J. B. R., Maycock, T. K., Waterfield, T., Yelekçi, O., Yu, R., and Zhou, B., Cambridge University Press, Cambridge, United Kingdom and New York, NY, USA, 1055–1210, <https://doi.org/10.1017/9781009157896.010>, 2021.
- ~~Dye, P. J., Gush, M. B., Everson, C. S., Jarman, C., Clulow, A., Mengistu, M., Geldenhuys, C. J., Wise, R., Scholes, R. J., Archibald, S., and Savage, M. J.: Water use in relation to biomass of indigenous tree species in woodland, forest and/or plantation conditions: Report to the Water Research Commission, 2008.~~
- Van Eimern, J., Karschon, R., Razumova, L. A., and Robertson, G. W.: Windbreaks and shelterbelts: report of a working group of the Commission for Agricultural Meteorology, 191 pp., 1964.
- Fauchereau, N., Trzaska, S., Rouault, M., and Richard, Y.: Rainfall variability and changes in Southern Africa during the 20th century in the global warming context, *Nat. Hazards*, 29, 139–154, <https://doi.org/10.1023/A:1023630924100>, 2003.
- Frouz, J., Dvorščík, P., Vávrová, A., Doušová, O., Kadochová, Š., and Matějček, L.: Development of canopy cover and woody vegetation biomass on reclaimed and unreclaimed post-mining sites, *Ecol. Eng.*, 84, 233–239, <https://doi.org/10.1016/j.ecoleng.2015.09.027>, 2015.
- van Genuchten, M. T.: A Closed-form Equation for Predicting the Hydraulic Conductivity of Unsaturated Soils, *Soil Sci. Soc. Am. J.*, 44, 892–898, <https://doi.org/10.2136/sssaj1980.03615995004400050002x>, 1980.
- ~~Gholz, H. L., Grier, C. C., Campbell, A. G., and Brown, A. T.: Equations for estimating biomass and leaf area of plants in the Pacific Northwest—research paper 41, Corvallis, Oregon, 1–38 pp., 1979.~~
- ~~Ghausi, S. A., Tian, Y., Zehe, E., and Kleidon, A.: Radiative controls by clouds and thermodynamics shape surface temperatures and turbulent fluxes over land, *Proc. Natl. Acad. Sci.*, 120, <https://doi.org/10.1073/pnas.2220400120>, 2023.~~
- Guderle, M. and Hildebrandt, A.: Using measured soil water contents to estimate evapotranspiration and root water uptake profiles – a comparative study, *Hydrol. Earth Syst. Sci.*, 19, 409–425, <https://doi.org/10.5194/hess-19-409-2015>, 2015.
- Guest, G., Bright, R. M., Cherubini, F., and Strømman, A. H.: Consistent quantification of climate impacts due to biogenic carbon storage across a range of bio-product systems, *Environ. Impact Assess. Rev.*, 43, 21–30, <https://doi.org/10.1016/j.eiar.2013.05.002>, 2013.
- Häckel, H.: Farbatlas Wetterphänomene, Ulmer, 1999.
- [Worldwide 'open access' tree functional attributes and ecological database: http://db.worldagroforestry.org/](http://db.worldagroforestry.org/), last access: 14 August 2023.
- Herbst, M., Eschenbach, C., and Kappen, L.: Water use in neighbouring stands of beech (*Fagus sylvatica* L.) and black alder (*Alnus glutinosa* (L.) Gaertn.), *Ann. For. Sci.*, 56, 107–120, <https://doi.org/10.1051/forest:19990203>, 1999.
- Hintermaier-Erhard, G. and Zech, W.: Wörterbuch der Bodenkunde, Enke, Stuttgart, 1997.
- ISO 11277:2002: Soil quality — Determination of particle size distribution in mineral soil material — Method by sieving and sedimentation — Technical Corrigendum 1, 2, 2002.
- IUSS Working Group: World Reference Base for Soil Resources. World Soil Resources Reports 106, 1–191 pp., 2014.
- Jackisch, C., ~~Angermann, L., Allroggen, N., Sprenger, M., Blume, T., Tronicke, J., and Zehe, E.: Form and function in hillslope hydrology: In situ imaging and characterization of flow-relevant structures, *Hydrol. Earth Syst. Sci.*, 21, 3749–3775, <https://doi.org/10.5194/hess-21-3749-2017>, 2017.~~
- ~~Jackisch, C., Knoblauch, S., Blume, T., Zehe, E., and Hassler, S. K.: Estimates of tree root water uptake from soil moisture profile dynamics, *Biogeosciences*, 17, 5787–5808, <https://doi.org/10.5194/bg-17-5787-2020>, 2020.~~
- Jahn, R., Blume, H. P., Asio, V., Spaargaren, O., and Schád, P.: Guidelines for soil description, Rome, Italy, 2006.
- ~~Johansson, T.: Dry matter amounts and increment in 21- to 91-year-old common alder and grey alder and some practical~~

- [implications, *Can. J. For. Res.*, 29, 1679–1690, <https://doi.org/10.1139/x99-126>, 1999.](https://doi.org/10.1139/x99-126)
- Jose, S.: Agroforestry for ecosystem services and environmental benefits: an overview, *Agrofor. Syst.*, 76, 1–10, <https://doi.org/10.1007/s10457-009-9229-7>, 2009.
- 915 ~~Kreutzer, K.: The Root system of the red alder, in: *Methods of productivity studies in root systems and rhizosphere organisms*, edited by: Ghilarov, M. S., Kovda, V. A., Novichkova-Ivanova, L. N., Rodin, L. E., and Sveshnikova, V. M., Nauka, Leningrad, 114–119, 1986.~~
- ~~Kutschera, L. and Lichtenegger, E.: *Wurzelatlas mitteleuropäischer Waldbäume und Sträucher*, Leopold Stocker Verlag, Graz, 2002.~~
- 920 Kuyah, S., Whitney, C. W., Jonsson, M., Sileshi, G. W., Öborn, I., Muthuri, C. W., and Luedeling, E.: Agroforestry delivers a win-win solution for ecosystem services in sub-Saharan Africa. A meta-analysis, *Agron. Sustain. Dev.*, 39, <https://doi.org/10.1007/s13593-019-0589-8>, 2019.
- Lal, R.: Soil organic matter and water retention, *Agron. J.*, 112, 3265–3277, <https://doi.org/10.1002/agj2.20282>, 2020.
- Mbow, C., Van Noordwijk, M., Luedeling, E., Neufeldt, H., Minang, P. A., and Kowero, G.: Agroforestry solutions to address
- 925 food security and climate change challenges in Africa, <https://doi.org/10.1016/j.cosust.2013.10.014>, 2014.
- McNaughton, K. G.: Effects of windbreaks on turbulent transport and microclimate, *Agric. Ecosyst. Environ.*, 22/23, 17–39, [https://doi.org/10.1016/0167-8809\(88\)90006-0](https://doi.org/10.1016/0167-8809(88)90006-0), 1988.
- Meadows, M. E.: The Cape Winelands, in: *Landscapes and Landforms of South Africa*. *World Geomorphological Landscapes*, edited by: Grab, S. and Knight, J., Springer, Cham., 103–109, https://doi.org/10.1007/978-3-319-03560-4_12, 2015.
- 930 Mualem, Y.: A new model for predicting the hydraulic conductivity of unsaturated porous media, *Water Resour. Res.*, 12, 513–522, <https://doi.org/10.1029/WR012i003p00513>, 1976.
- Muthuri, C. W., Ong, C. K., Black, C. R., Mati, B. M., Ngumi, V. W., and Van-Noordwijk, M.: Modelling the effects of leafing phenology on growth and water use by selected agroforestry tree species in semi-arid Kenya, *L. Use Water Resour. Res.*, 4, 1–11, 2004.
- 935 Nägeli, W.: Untersuchungen über die Windverhältnisse im Bereich von Windschutzstreifen, in: *Mitteilungen der Schweizerischen Anstalt für das forstliche Versuchswesen*, edited by: Burger, H., Beer, Zürich, 223–276, 1943.
- Ndebele, N. E., Grab, S., and Turasie, A.: Characterizing rainfall in the south-western Cape, South Africa: 1841–2016, *Int. J. Climatol.*, 40, 1992–2014, <https://doi.org/10.1002/joc.6314>, 2020.
- Peters, A.: Reply to comment by S. Iden and W. Durner on “Simple consistent models for water retention and hydraulic
- 940 conductivity in the complete moisture range,” *Water Resour. Res.*, 50, 7535–7539, <https://doi.org/10.1002/2014WR016107>, 2014.
- Raumonen, P.: Quantitative structure models of single trees from laser scanner data: Instructions for MATLAB-software TreeQSM, 2017.
- Raumonen, P., Kaasalainen, M., Markku, Å., Kaasalainen, S., Kaartinen, H., Vastaranta, M., Holopainen, M., Disney, M., and
- 945 Lewis, P.: Fast automatic precision tree models from terrestrial laser scanner data, *Remote Sens.*, 5, 491–520, <https://doi.org/10.3390/rs5020491>, 2013.
- Rosenstock, T. S., Dawson, I. K., Aynekulu, E., Chomba, S., Degrande, A., Fornace, K., Jamnadass, R., Kimaro, A., Kindt, R., Lamanna, C., Malesu, M., Mausch, K., McMullin, S., Murage, P., Namoi, N., Njenga, M., Nyoka, I., Paez Valencia, A. M., Sola, P., Shepherd, K., and Steward, P.: A Planetary Health Perspective on Agroforestry in Sub-Saharan Africa, *One Earth*,
- 950 1, 330–344, <https://doi.org/10.1016/j.oneear.2019.10.017>, 2019.
- [San-Miguel-Ayanz, J., de Rigo, D., Caudullo, G., Houston Durrant, T., and Mauri, A. \(Eds.\): *European atlas of forest tree species*, Publications Office of the European Union, Luxembourg, <https://doi.org/10.2760/776635>, 2016.](https://doi.org/10.2760/776635)
- Schumacher, J. and Christiansen, J. R.: LiDAR Applications to Forest-Water Interactions., in: *Forest-water interactions*, vol. 240, edited by: Levia, D. F., Canadell, J. G., Díaz, S., Heldmaier, G., Jackson, R. B., Schulze, E.-D., Sommer, U., and Wardle,

- 955 D. A., Springer, Cham, Switzerland, 87–112, 2020.
- Shao, Y. (Ed.): *Physics and Modelling of Wind Erosion*, Springer Netherlands, Dordrecht, <https://doi.org/10.1007/978-1-4020-8895-7>, 2008.
- Sheppard, J. P., Bohn Reckziegel, R., Borrass, L., Chirwa, P. W., Cuaranhua, C. J., Hassler, S. K., Hoffmeister, S., Kestel, F., Maier, R., Mälicke, M., Morhart, C., Ndlovu, N. P., Veste, M., Funk, R., Lang, F., Seifert, T., du Toit, B., and Kahle, H.-P.:
- 960 *Agroforestry: An Appropriate and Sustainable Response to a Changing Climate in Southern Africa?*, *Sustainability*, 12, 6796, <https://doi.org/10.3390/su12176796>, 2020a.
- Sheppard, J. P., Chamberlain, J., Agúndez, D., Bhattacharya, P., Chirwa, P. W., Gontcharov, A., Sagona, W. C. J., Shen, H. long, Tadesse, W., and Mutke, S.: *Sustainable Forest Management Beyond the Timber-Oriented Status Quo: Transitioning to Co-production of Timber and Non-wood Forest Products—a Global Perspective*, *Curr. For. Reports*, 6, 26–40,
- 965 <https://doi.org/10.1007/s40725-019-00107-1>, 2020b.
- [Sheppard, J. P., Larysch, E., Cuaranhua, C. J., Schindler, Z., du Toit, B., Malherbe, G. F., Kunneke, A., Morhart, C., Bohn Reckziegel, R., Seifert, T., and Kahle, H.-P.: Assessment of biomass and carbon storage of a *Populus simonii* windbreak located in the Western Cape Province, South Africa, *Agrofor. Syst.*, <https://doi.org/10.1007/s10457-023-00940-1>, 2024.](https://doi.org/10.1007/s10457-023-00940-1)
- Shi, L., Feng, W., Xu, J., and Kuzyakov, Y.: *Agroforestry systems: Meta-analysis of soil carbon stocks, sequestration*
- 970 *processes, and future potentials*, *L. Degrad. Dev.*, 29, 3886–3897, <https://doi.org/10.1002/ldr.3136>, 2018.
- Sileshi, G. W., Akinnifesi, F. K., Mafongoya, P. L., Kuntashula, E., and Ajayi, O. C.: *Potential of Gliricidia-Based Agroforestry Systems for Resource-Limited Agroecosystems*, in: *Agroforestry for Degraded Landscapes*, Springer Singapore, Singapore, 255–282, https://doi.org/10.1007/978-981-15-4136-0_9, 2020.
- [Smith, M. M., Bentrup, G., Kellerman, T., MacFarland, K., Straight, R., and Ameyaw, Lord: Windbreaks in the United States: A systematic review of producer-reported benefits, challenges, management activities and drivers of adoption, *https://doi.org/10.1016/j.agsy.2020.103032*, 2021.](https://doi.org/10.1016/j.agsy.2020.103032)
- 975 [Stellenbosch Weather: *http://weather.sun.ac.za/*, last access: 3 April 2023.](http://weather.sun.ac.za/)
- Thomas, S. C. and Martin, A. R.: *Carbon Content of Tree Tissues: A Synthesis*, *Forests*, 3, 332–352, <https://doi.org/10.3390/f3020332>, 2012.
- 980 Veste, M., Littmann, T., Kunneke, A., du Toit, B., and Seifert, T.: *Windbreaks as part of climate-smart landscapes reduce evapotranspiration in vineyards, Western Cape Province, South Africa*, *Plant, Soil Environ.*, 66, 119–127, <https://doi.org/10.17221/616/2019-PSE>, 2020.
- Wilkes, P., Lau, A., Disney, M., Calders, K., Burt, A., Gonzalez de Tanago, J., Bartholomeus, H., Brede, B., and Herold, M.: *Data acquisition considerations for Terrestrial Laser Scanning of forest plots*, *Remote Sens. Environ.*, 196, 140–153,
- 985 <https://doi.org/10.1016/j.rse.2017.04.030>, 2017.
- Wilson, M. H. and Lovell, S. T.: *Agroforestry-The next step in sustainable and resilient agriculture*, *Sustain.*, 8, <https://doi.org/10.3390/su8060574>, 2016.
- ~~[Worldwide 'open access' tree functional attributes and ecological database: *http://db.worldagroforestry.org/*, last access: 14 August 2023.](http://db.worldagroforestry.org/)~~
- 990 Zehe, E., Maurer, T., Ihringer, J., and Plate, E.: *Modeling water flow and mass transport in a loess catchment*, *Phys. Chem. Earth, Part B Hydrol. Ocean. Atmos.*, 26, 487–507, [https://doi.org/10.1016/S1464-1909\(01\)00041-7](https://doi.org/10.1016/S1464-1909(01)00041-7), 2001.